



MSU Graduate Theses

Spring 2018


Investigation into the Role of Platelet Derived Growth Factor (PDGF) in Type I Collagen Glomerulopathy

Isaac C. Springer

Missouri State University, Springer4017@live.missouristate.edu

As with any intellectual project, the content and views expressed in this thesis may be considered objectionable by some readers. However, this student-scholar's work has been judged to have academic value by the student's thesis committee members trained in the discipline. The content and views expressed in this thesis are those of the student-scholar and are not endorsed by Missouri State University, its Graduate College, or its employees.

Follow this and additional works at: <https://bearworks.missouristate.edu/theses>

 Part of the [Animal Diseases Commons](#), [Animals Commons](#), [Physiological Processes Commons](#), and the [Reproductive and Urinary Physiology Commons](#)

Recommended Citation

Springer, Isaac C., "Investigation into the Role of Platelet Derived Growth Factor (PDGF) in Type I Collagen Glomerulopathy" (2018). *MSU Graduate Theses*. 3273.
<https://bearworks.missouristate.edu/theses/3273>

This article or document was made available through BearWorks, the institutional repository of Missouri State University. The work contained in it may be protected by copyright and require permission of the copyright holder for reuse or redistribution.

For more information, please contact [BearWorks@library.missouristate.edu](mailto: BearWorks@library.missouristate.edu).

**INVESTIGATION INTO THE ROLE OF PLATELET DERIVED GROWTH
FACTOR (PDGF) IN TYPE I COLLAGEN GLOMERULOPATHY**

A Masters Thesis

Presented to

The Graduate College of
Missouri State University

In Partial Fulfillment

Of the Requirements for the Degree
Master of Science, Cell and Molecular Biology

By

Isaac Springer

May 2018

Copyright 2018 by Isaac Charles Springer

INVESTIGATION INTO THE ROLE OF PLATELET DERIVED GROWTH FACTOR (PDGF) IN TYPE I COLLAGEN GLOMERULOPATHY

Biomedical Sciences

Missouri State University, May 2018

Masters of Science

Isaac Springer

ABSTRACT

Progressive accumulation of collagen and extracellular matrix (ECM) proteins within renal glomeruli have implications for or result in renal fibrosis and glomerulosclerosis, with both events culminating in renal failure. To model this accumulation the *Colla2-deficient* mouse model was used. The *Colla2-deficient* mouse model is characterized by a mutation in the $\alpha 2(I)$ chain, preventing incorporation into the type I collagen molecule. As a result, an $\alpha 1(I)$ collagen chain incorporates into the collagen triple helix forming homotrimeric type I collagen, as opposed to heterotrimeric type I collagen. This change is due to the secondary wound healing response in response to ECM accumulation, fibrosis, or damage. Transforming growth factor-beta (TGF- β) has been studied within this model and demonstrated it was not the initiating molecule in collagen deposition. This study looks at Tumor Necrosis Factor-Alpha (TNF- α) and Platelet Derived Growth Factor (PDGF) as potential mediators of this hypothesized secondary wound healing response. TNF- α is an inflammatory cytokine produced following tissue damage, released by mesangial cells, and has been shown to induce epithelial-to-mesenchymal transition (EMT). Recently, PDGF receptors and ligand upregulation has been shown in other mouse models of renal fibrosis. However, TNF- α showed no differential staining upon Picrosirius Red (PSR) between experimental and control groups. PDGFR- $\beta\beta$ and PDGF-BB displayed differential labeling in *Colla2-deficient* in comparison to age matched wild type animals. The results for PDGF-DD mice were less conclusive when comparing the *Colla2-deficient* mice to that of their wild type counterparts.

KEYWORDS: renal fibrosis, homotrimeric type I collagen, *Colla2-deficient* mouse model, platelet derived growth factor, glomeruli, secondary wound healing.

This abstract is approved as to form and content

Amanda Brodeur, MD/PhD
Chairperson, Advisory Committee
Missouri State University

**INVESTIGATION INTO THE ROLE OF PLATELET DERIVED GROWTH
FACTOR (PDGF) IN TYPE I COLLAGEN GLOMERULOPATHY**

By

Isaac Springer

A Masters Thesis
Submitted to the Graduate College
Of Missouri State University
In Partial Fulfillment of the Requirements
For the Degree of Masters of Science; Cellular and Molecular Biology

May 2018

Approved:

Amanda Brodeur, MD/PhD

Lyon Hough, PhD

Amy Hulme, PhD

Julie Masterson, PhD: Dean, Graduate College

In the interest of academic freedom and the principle of free speech, approval of this thesis indicates the format is acceptable and meets the academic criteria for the discipline as determined by the faculty that constitute the thesis committee. The content and views expressed in this thesis are those of the student-scholar and are not endorsed by Missouri State University, its Graduate College, or its employees.

ACKNOWLEDGEMENTS

I would like to thank the following people for their help with IHC and sectioning during the course of my graduate studies: Whitney Yarnell, Zach Sims, Amanda Harris, Jake Sharon, Ruth Ehie, Grant Beck, Nicole Hitchcock, Randi Kerr, Cody Likens, Kelli Rosen, and Trevor Koelling. A special thanks to Whitney Yarnell, Jake Sharon, Amanda Harris, Nicole Hitchcock, Randi Kerr, Cody Likens, and Grant Beck. You were a part of the project from the beginning and this would not have been possible without you. I wish each of you success in whatever the future holds. Dr. Brodeur, you have been inspiring, encouraging, and a mentor, but more than any of these, you believed in me. I have an immense amount of gratitude for the time and effort you have invested into my life, thank you.

I dedicate this thesis to my wife Hannah, my family, and all of the graduate students that were along for the ride. Hannah, you have been my rock through these last two years. Mom and Dad, from a young age you taught me what it meant to put my best foot forward in everything I do. Jacob and Nathan, thank you for the encouragement and support, I have always looked up to both of you. CMB graduate students, I will never forget the time we spent in the Professional building at Missouri State University, you will forever be friends.

TABLE OF CONTENTS

Introduction.....	1
Clinical Significance.....	1
Collagen and <i>Colla2-deficient</i> Mouse Model.....	2
Glomerular Structure and Development.....	5
Characterization of Type I Collagen Glomerulopathy.....	8
Deficient Degradation of Homotrimeric Type I Collagen.....	12
Investigation into the Potential Role of TGF- β in <i>Colla2-deficient</i> Mice.....	19
Investigation into the Potential Role of TNF- α in <i>Colla2-deficient</i> Mice.....	26
Investigation into the Potential Role of PDGF in <i>Colla2-deficient</i> Mice.....	30
Aims.....	33
Materials & Methods.....	35
Picro Sirius Red (PSR) Staining.....	35
Tissue and Histology (TNF- α).....	35
Lesion Scoring (TNF- α).....	36
Morphometry Mapping.....	37
Histology (PDGF).....	37
Immunohistochemical (IHC) Labeling (PDGF).....	37
Results.....	39
Tumor Necrosis Factor - Alpha.....	39
Platelet Derived Growth Factor – Receptor $\beta\beta$, Ligand -BB, Ligand -DD.....	46
Discussion.....	53
Tumor Necrosis Factor – Alpha.....	53
Platelet Derived Growth Factor.....	54
Core Fucosylation Regulation – PDGF & TGF- β 1.....	55
Future Directions.....	56
References.....	58
Appendix.....	64

LIST OF TABLES

Table 1. <i>Colla2-deficient</i> mice demonstrate albuminuria as compared with wild type animals.....	18
Table 2. Mean Lesion Score for Wild Type and <i>Colla2-deficient</i> Mice	45

LIST OF FIGURES

Figure 1. Heterotrimeric and Homotrimeric Type I Collagen.	6
Figure 2. Structure of Collagen.	7
Figure 3. Medullary Section of Kidney Structure.	9
Figure 4. Cross Section and Internal Structure of a Glomerulus.	10
Figure 5. Deposition of type I collagen in heterozygous and <i>Colla2-deficient</i> glomeruli.	13
Figure 6. Initiation of type I collagen deposition in glomeruli occurs postnatally.	14
Figure 7. The type I collagen glomerulopathy in heterozygous mice demonstrate a gene dose effect (* <i>P</i> <0.0001) that is progressive with age (** <i>P</i> <0.0001).	15
Figure 8. The type I collagen glomerulopathy initiates postnatally and glomeruli sequentially become affected in a centrifugal pattern from the juxtamedullary (jm) to the cortical (c) region in a distribution consistent with glomerular maturation and initiation of function.	16
Figure 9. Electron Microscopy of Glomeruli from Wild Type and <i>Colla2-deficient</i> Mice.	17
Figure 10. Identification of type I collagen homotrimer in wildtype (+/+) (A,D,G,J), heterozygous (+/-) (B,E,H,K) and homozygous (-/-)(C,F,I,L) glomeruli.	20
Figure 11. Quantitative RT-PCR steady-state mRNA expression.	21
Figure 12. MMP-2, -3, and -9 Quantitative RT-PCR.	22
Figure 13. <i>Colla2-deficient</i> (-/-) glomeruli demonstrate parietal epithelial cell (PEC) EMT at 1-month of age.	27
Figure 14. TGF-β1 steady-state mRNA and protein are not upregulated in homotrimeric type I collagen glomerulopathy.	28
Figure 15. <i>Colla2-deficient/Smad3-deficient</i> glomeruli demonstrate homotrimeric type I collagen deposition.	29
Figure 16. Simplification of main molecules involved in PDGF-PDGFR interactions. ...	34

Figure 17. Deposition of Type I Collagen in Untreated Wildtype Mice.....	41
Figure 18. Deposition of Type I Collagen in Treated Wildtype Mice.	42
Figure 19. Deposition of Type I Collagen in Untreated <i>Colla2-deficient</i> Mice	43
Figure 20. Deposition of Type I Collagen in Treated <i>Colla2-deficient</i> Mice	44
Figure 21. Picrosirius Red (PSR) Stain of Five Wild Type and Five <i>Colla2-deficient</i> Mice	49
Figure 22. 40x Magnification of PDGFR- $\beta\beta$ Labeling in Glomeruli of Wild Type and <i>Colla2-deficient</i> Mice.	50
Figure 23. 40x Magnification of PDGF-BB Labeling in Glomeruli of Wild Type and <i>Colla2-deficient</i> Mice.	51
Figure 24. 40x Magnification of PDGF-DD Labeling in Glomeruli of Wild Type and <i>Colla2-deficient</i> Mice.	52
Figure A1. Core fucosylation was down-regulated and the pericyte-myofibroblast transition was inhibited upon FUT8 knockdown <i>in vitro</i>	64
Figure A2. The pericyte-myofibroblast transition was inhibited and RIF was reduced upon FUT8 knockdown <i>in vivo</i>	65
Figure A3. Core fucosylation regulates the pericyte-myofibroblast transition through both the TGF β /Smad2/3 and PDGF/ERK1/2 pathways <i>in vitro</i>	66
Figure A4. Core fucosylation regulates transforming growth factor b (TGF-b) and platelet-derived growth factor (PDGF) signaling pathways in the pathophysiology of peritoneal fibrosis.....	67

INTRODUCTION

Clinical Significance

A Center for Disease Control (CDC) report from 2017 found morbidity rates from chronic kidney disease (CKD) estimated at 30 million. This indicated that 15% of the United States adult population is suffering from some form of CKD. 96% of individuals living with mild CKD are unaware of this disease.¹ Risk factors for developing CKD include: diabetes, high blood pressure, high fat diet, smoking, and others.² Signs and symptoms of CKD include: nausea, loss of appetite, vomiting, fatigue or weakness, change in frequency of urination, muscle twitches or cramps, chest pain, shortness of breath, high blood pressure, and many more. However, these signs normally present after it is too late to reverse the effects of CKD.²

Many complications can arise from having CKD, for example, an increase in heart and blood vessel disease.¹ In addition, anemia, fluid retention (swelling), an increase in potassium levels (hyperkalemia), reduced immune response, and others are also complications associated with CKD.² However, these complications can be avoided by selecting wise food options. Eating food with less potassium, less added salt, and less phosphorous can all help in reducing chances of developing CKD.² However, if a patient does present with CKD there are treatment options to improve health. Medication is one route, this includes medication for: blood pressure, cholesterol, anemia, and increase in fluid (swelling). Calcium and vitamin D supplement may be given if bone integrity is affected.²

CKD is progressive and ultimately will develop into End Stage Renal Disease (ESRD). The full manifestation of both of these diseases is renal failure. Development of renal failure results in dialysis treatment and kidney transplantation.¹ CKD and ESRD is very expensive to treat and places a large burden on Medicare. The estimated cost of treating patients with CKD and ESRD in America, as reported by the United States Renal Data System (USRDS), is 100 billion dollars per year. 64 billion of these dollars are being used to treat individuals with CKD, and another 34 billion are being used for patients with ESRD. The combined costs of CKD and ESRD alone make this an urgent issue in the United States.³

Studying fibrosis and kidney disease utilizes the use of mouse models. In this study, the *Colla2-deficient* mouse model was used.

Collagen and *Colla2-deficient* Mouse Model

Originally, the *Colla2-deficient* was termed osteogenesis imperfecta model, as it was used to study musculoskeletal malformations within mice.⁴ A decrease in bone integrity characterizes COL1A1/2-related osteogenesis imperfecta with four distinct varieties. The bones of individuals are highly brittle and can fracture with little to no trauma.⁵ However, for this study, the *Colla2-deficient* mouse model is being used to study homotrimeric type I collagen glomerulopathy.

There are at least 16 types of collagen in the human body⁶, but type I collagen is the most abundant.⁷ Collagen is a structural protein seen in the extracellular matrix (ECM). It functions as a scaffolding protein for blood vessels throughout the body, makes up a large percentage of bone density, and is involved in the secondary wound healing response to repair tissue damage. Type I collagen starts out as pro α 2 and pro α 1 chains.

These chains have their carboxy-peptide regions cleaved which allows the chains to incorporate into a helix conformation.⁸ Resulting in collagen transforming from a pro-collagen to mature collagen form. Type I collagen is a triple helix composed of three interacting alpha chains and exists naturally in two isotypes (Figure 1). The most abundant is the type I collagen heterotrimer composed of two $\alpha 1$ chains and an $\alpha 2$ chain. These chains are synthesized as pro-collagen fibrils, pro $\alpha 1$ (I) and pro $\alpha 2$ (I) respectively (Figure 2) and are encoded for by the COL1A1 and COL1A2 genes. Figure 2 illustrates heterotrimeric type I collagen as a right handed triple helix. Each chain making up the homotrimer is characterized by a Gly-Xaa-Yaa repeat, with glycine packed in the middle of the right handed triple helix to coil heterotrimeric type I collagen.⁹

The COL1A1 gene is on the 11th chromosome and the COL1A2 gene is located on the 6th chromosome in *Mus musculus* or mouse.^{10,11} The homotrimeric type I collagen is composed, exclusively, of $\alpha 1$ chains. The type I collagen homotrimer is seen in very small amounts physiologically, and is present in adult skin, embryological development, and during the wound healing response.⁷

The COL1A2 mouse model is characterized by a homozygous mutation found within the COL1A2 gene. Because of this, these mice synthesize mutated pro $\alpha 2$ (I) chains that are unable to incorporate into the triple helix. This spontaneous mutation has resulted in a DNA deletion within the carboxy-peptide encoding region. This spontaneous mutation is responsible the loss of interaction between the $\alpha 2$ chain and its $\alpha 1$ chain counterparts.⁷ Since the $\alpha 2$ chains are not incorporated into type I collagen, they are replaced with an $\alpha 1$ chain, thereby, producing homotrimeric type I collagen.¹² The *Colla2-deficient* mouse model exclusively synthesizes homotrimeric type I collagen in

the homozygous affected mice. Type I collagen, specifically the homotrimer, is deposited in the mesangial matrix of glomeruli in these *Colla2-deficient* mice.⁷

A negative feedback mechanism controls synthesis of the COL1A2 and COL1A1 genes through the cleavage of the pro α 2(I) carboxy-peptide region, the area responsible for interaction between α 2 and α 1 chains. Upon cleavage there is a translocation of this pro α 2 carboxy-peptide region to the nucleus where it downregulates the transcription of not only the COL1A2 gene, but also the COL1A1 gene.⁸ Cleavage of the carboxy-peptide region has been shown to decrease the assembly of collagen. The mutation in the carboxy-peptide region of the pro α 2(I) within the *Colla2-deficient* mouse model no longer allows this cleavage to occur, this suggests that the carboxy-peptide cleavage deficiency within the α 2 chain could allow an overproduction of the homotrimeric type I collagen isotype.¹³ However, overproduction of collagen could also be due to a decrease in the degradation of homotrimeric type I collagen by matrix metalloproteinases (MMPs).

Recent studies have shown that heterotrimeric type I collagen is more vulnerable to degradation than homotrimeric type I collagen. Homotrimeric type I collagen is actually said to be resistant to degradation by MMPs.¹⁴ It was hypothesized that not only an increase in synthesis of homotrimer but also a decrease in degradation of the homotrimer is contributing to the pathology of homotrimeric type I collagen glomerulopathy in the *Colla2-deficient* mice.⁷

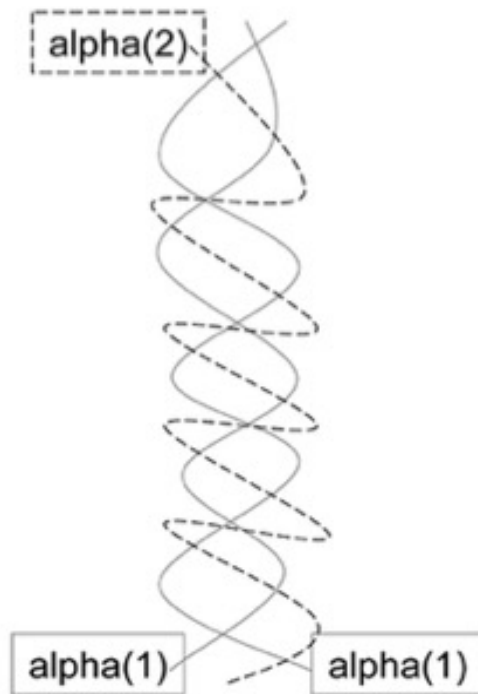
The COL1A2 mouse model offers an excellent way to study homotrimeric type I collagen and its effects within the kidney. Comparison of *Colla2-deficient* mice and wild type mice help characterize the role of homotrimeric type I collagen in wild type vs. *Colla2-deficient* mice. Lastly, the *Colla2-deficient* mouse model will help define the

role of $\alpha 2(I)$ chains functionality in collagen.⁴

Glomerular Structure and Development

Collagen deposition, seen within the *Colla2-deficient* mouse model, occurs in the glomeruli of the kidneys. Glomeruli are composed of mesangial cells, epithelial cells, referred to as podocytes, and endothelial cells. Endothelial cells form a boundary between blood vessels and tissue, however, glomerular endothelial cells are more specialized. They are highly fenestrated with the fenestrations making up 30-50% of their overall surface area. Glomerular endothelial cells have a role in the ability of nephron to produce filtrate at such an efficient rate.¹⁷ The fenestrations of endothelial cells are equivalent to the filtration slits created by podocytes. Epithelial cells, i.e. podocytes, are found attached to glomerular capillaries. Podocytes interdigitate with one another to form filtration slits contributing to the efficiency of ultrafiltrate production.¹⁸ Mesangial cells comprise greater than 30-40% of the entire glomerulus.¹⁹ Mesangial cells have various functions from phagocytosis, removing debris from filtration to slits, aiding in maintenance of the glomerular filtration rate (GFR), and their ability to produce extracellular matrix (ECM) proteins. ECM proteins include collagen, elastin, fibronectin, and laminin.²⁰ ECM proteins are responsible for cellular scaffolding and formation of the glomerular basement membrane.²¹ A cross section of a glomerulus is provided (Figure 3) and shows the different cells type and their organization within the Bowman's capsule. A Bowman's capsule houses an individual glomerulus and is connected to the tubular system. Glomeruli are what allow the functional unit of the kidney, the nephron (Figure 4), to filter blood and produce urine.

Heterotrimeric



Homotrimeric

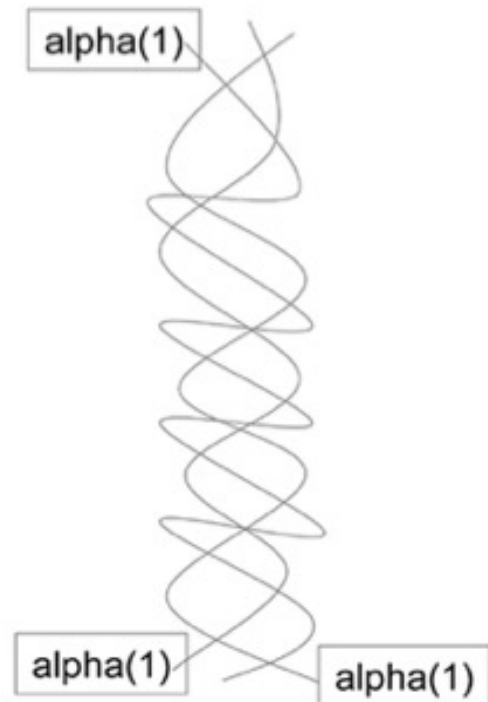


Figure 1. Heterotrimeric and Homotrimeric Type I Collagen.

Type I collagen exists as two isotypes; heterotrimeric and homotrimeric type I collagen. The heterotrimer is seen in greater abundance throughout the body and is made up of one $\alpha 2(I)$ chain and two $\alpha 1(I)$ chains. The homotrimer is seen in wound healing and embryological development. The homotrimer is made up of three $\alpha 1(I)$ chains. Figure created by Amanda Brodeur, MD/PhD.

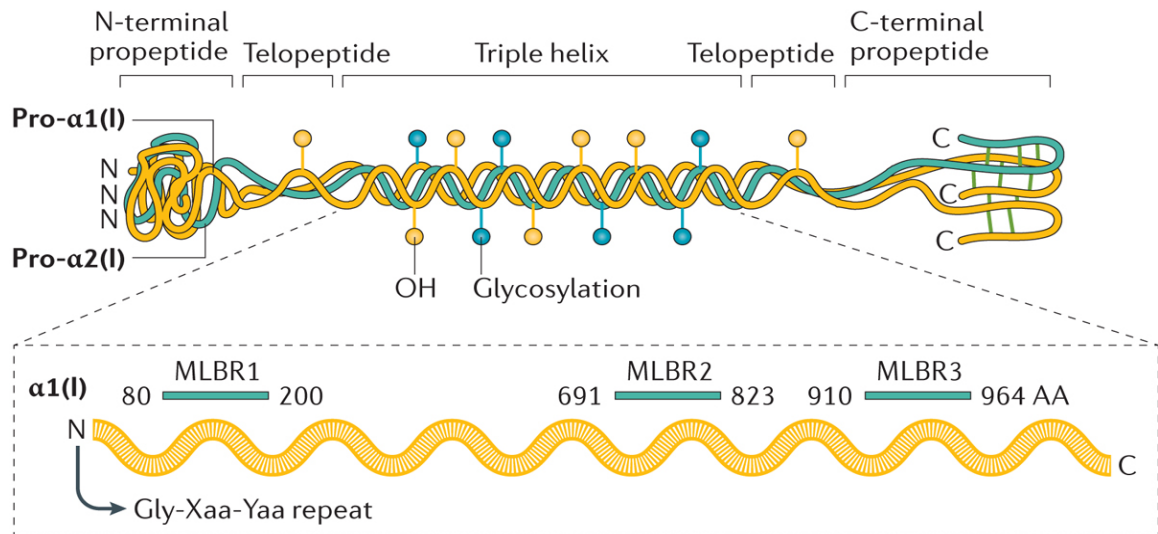


Figure 2. Structure of Collagen.

Type I collagen is a heterotrimer composed of two $\alpha 1$ and one $\alpha 2$ left-handed polyproline II-like chains that are assembled into a right-handed triple helix. It is synthesized as a procollagen, containing both amino-terminal and carboxyl-terminal propeptide sequences, which are proteolytically cleaved by specific proteases (a disintegrin and metalloproteinase with thrombospondin motifs 2 (ADAMTS2) and bone morphogenetic protein 1 (BMP1), respectively) that recognize a sequence in the telopeptides, that is, p.Pro161Gln162 in $\alpha 1(I)$ and p.Ala79Gln80 in $\alpha 2(I)$ for the N-terminal cleavage sites, and p.Ala1218Asp1219 and p.Ala1119Asp1120 for the C-terminal cleavage sites.¹⁵ The sequence of each collagen chain is characterized by Gly-Xaa-Yaa repeats (in which X and Y can be any amino acid (AA) but are most often proline and hydroxyproline). Glycine is required at every third position and is tightly packed at the center of the triple helical structure. Collagen contains ~20% proline residues. The post-translational 4-hydroxylation of most prolines in the Yaa position is required for triple helical stability.¹⁶ Along the $\alpha 1$ -chain, specific regions that are relevant for the interaction of collagen with other collagen molecules or with extracellular matrix proteins were identified, namely, major ligand-binding region (MLBR).⁹

Collagen is an important protein in renal function. Type 4 collagen is the primary component of the basement membrane; however, in this study, type I collagen is the collagen of interest and is found supporting vasculature in healthy kidney, no collagen is found within glomeruli. However, type I collagen has been seen to be synthesized upon renal injury or damage to the glomerulus. Furthermore, cultured mesangial cells have been shown to produce ECM, primarily type I collagen, but also, types III, IV, and V collagens.²⁰

Mice are born with numerous (2,000-2,500²²) glomeruli at birth, but these glomeruli are not all functional. The glomeruli follow a development timeline from day zero to day 21. Glomeruli first develop in the juxtamedullary region and then develop in a centrifugal pattern outward towards the cortex.²³⁻²⁵ The glomeruli in the cortex fully develop at day 21. Humans and other mammals exhibit a similar centrifugal development pattern.²⁵⁻²⁷

Characterization of Type I Collagen Glomerulopathy

Homogenous material was present in renal glomeruli of *Colla2-deficient* mice when analyzed histologically.⁷ Picosirius Red (PSR) was used to evaluate if this accumulation was indeed collagen. Glomeruli from *Colla2-deficient* mice stained positive for PSR, showing that type I or type III collagen was present in the glomeruli of *Colla2-deficient* mice.⁴ It was also shown that heterozygous animals had small amounts of PSR positive glomeruli (Figure 5). Electron microscopy (EM) was used to further localize the deposition of collagen in the glomerulus. EM showed that collagen had been deposited in the renal mesangium.⁷ It was unknown if type I or type III collagen was deposited in the renal mesangium, antibody labeling was used to detect the pro α 1(I)

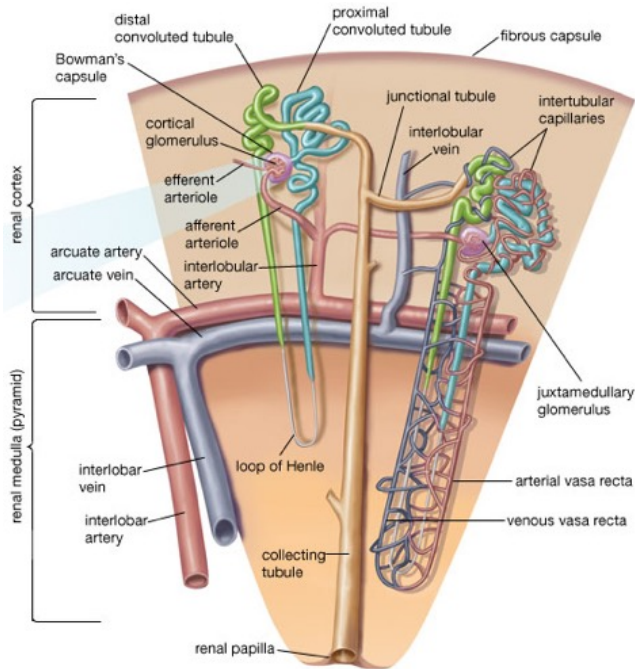


Figure 3. Medullary Section of Kidney Structure.

Kidneys contain approximately twelve medullary regions and each region has numerous nephrons woven throughout the cortex and medullary pyramid. The Bowman's capsule housing the glomerulus is found in the cortical region along with the Proximal Convoluted Tubule (PCT) and Distal Convoluted Tubule (DCT). The Loop of Henle extends into the salty medullary region where water is taken out of the tubule network and resorbed into the tissue. The nephron is the main urine filtration unit.²⁸

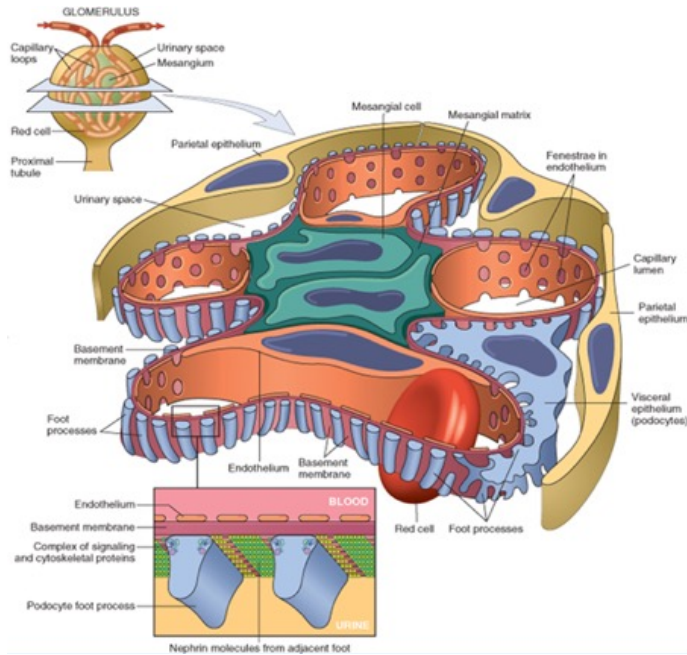


Figure 4. Cross Section and Internal Structure of a Glomerulus.

Filtration takes place, initially, in the glomerulus. The glomerulus is comprised of three major cell types: mesangial, epithelial, and endothelial. The mesangial cells are seen in the middle of the image in green with purple nuclei. The visceral epithelium (podocytes) are seen in light blue along with their foot processes that interdigitate with one another. and capillary loops are seen as open spaces surround by fenestrated endothelium in orange. The basement membrane is seen in dark pink and finally the Bowman's capsule is seen in yellow and is made up of parietal epithelium.²⁹

chain and the pro α 1(III) chain. Immunohistochemistry (IHC) showed antibody labeling for the pro α 1(I) chain and not the pro α (III) chain indicating that the homogenous material accumulated in the renal mesangium was in fact type I collagen.⁴

Further study demonstrated that heterozygous animals were affected in a gene dose dependent manner.¹⁴ The deposition of type I collagen occurred early within the development process, as early as one-week of age in the juxtamedullary region. In addition, at the end of glomerular development, around one month of age there was collagen deposited in glomeruli in all regions of the kidney (Figure 6). Approximately 55% of all glomeruli in *Colla2-deficient* mice were affected in mice two weeks of age in comparison to only 8% of glomeruli in heterozygous mice. At the end of glomerular maturation, one-month of age, PSR positive staining was present in 95% of *Colla2-deficient* mice in comparison to 54% of heterozygous mice (Figure 7). The pattern of collagen deposition followed glomerular maturation. Collagen is first deposited in the glomeruli located in the juxtamedullary region followed by the cortical region at one-month (Figure 8). It was also shown that the type I collagen glomerulopathy was progressive with age.⁷

Electron microscopy further showed the extent of collagen deposition and exhibited collagen deposition in the mesangial matrix and in the subendothelial spaces, increasing the distance between endothelial cells and the glomerular basement membrane. Podocyte effacement was also observed potentially affecting the integrity of the glomeruli (Figure 9). Podocyte effacement is characterized by the fusion or retraction of podocyte foot processes.²⁵ Podocyte effacement paired with proteinuria is indicative

that collagen deposition is leading to glomerular injury and impairment of renal function.⁷

Albumin and creatinine levels were analyzed to determine if the collagen deposition had pathologic significance. A mean of 38.19 μg albumin/mg creatinine for *Colla2-deficient* mice was observed, compared to 0.50 μg albumin/mg creatinine for wild type mice (Table 1).⁷

Deficient Degradation of Homotrimeric Type I Collagen

To prove that *Colla2-deficient* mice were only making homotrimeric collagen and to determine which isotype of type I collagen was deposited in heterozygous mice, immunohistochemical analysis of $\alpha 1(\text{I})$ and $\alpha 2(\text{I})$ was performed. IHC analysis revealed that $\alpha 1(\text{I})$ and $\alpha 2(\text{I})$ were present in the vasculature of the wild type mice, however, no $\alpha 2(\text{I})$ antibody was present within the glomeruli of the heterozygous and homozygous mice. In contrast, $\alpha 1(\text{I})$ chain was present in glomeruli of both heterozygous and homozygous *Colla2-deficient* mice (Figure 10).¹⁴

To determine if the deposition of homotrimeric type I collagen was in response to increased $\text{pro}\alpha 1(\text{I})$ and $\text{pro}\alpha 2(\text{I})$ gene expression, whole kidneys were analyzed via RT-PCR from all three genotypes of mice: wild type, heterozygous, and homozygous affected. Different age groups were evaluated, one-week, two-weeks, and one-month of age. mRNA levels for $\text{pro}\alpha 1(\text{I})$ were higher in *Colla2-deficient* mice at one month in comparison to wild type and heterozygous mice. This was further confirmed as glomeruli isolations from these mice were evaluated via RT-PCR and showed similar findings to that of the whole kidney isolates (Figure 11).¹⁴ Based on IHC it would be expected that COL1A1 mRNA would increase in heterozygous animals, however, this increase was not

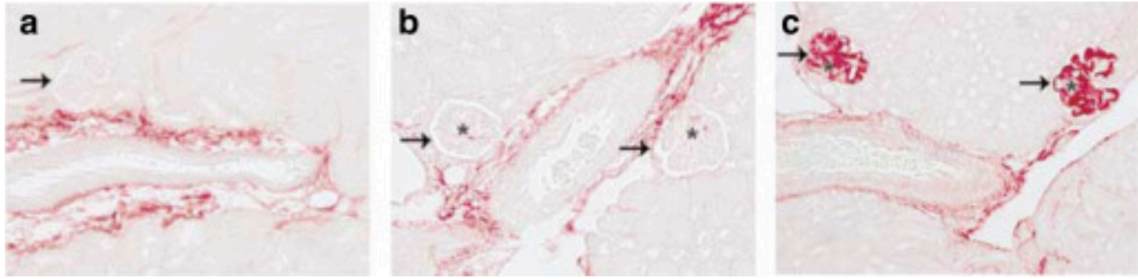


Figure 5. Deposition of type I collagen in heterozygous and *Colla2*-deficient glomeruli. Picosirius red-stained sections of (a) wild type (lesion score 0), (b) heterozygous (lesion score 1), and (c) *Colla2*-deficient (lesion score 4) kidneys from 1-month-old mice. Arrows indicate glomeruli. Asterisks denote affected (Picosirius red+) glomeruli.⁷

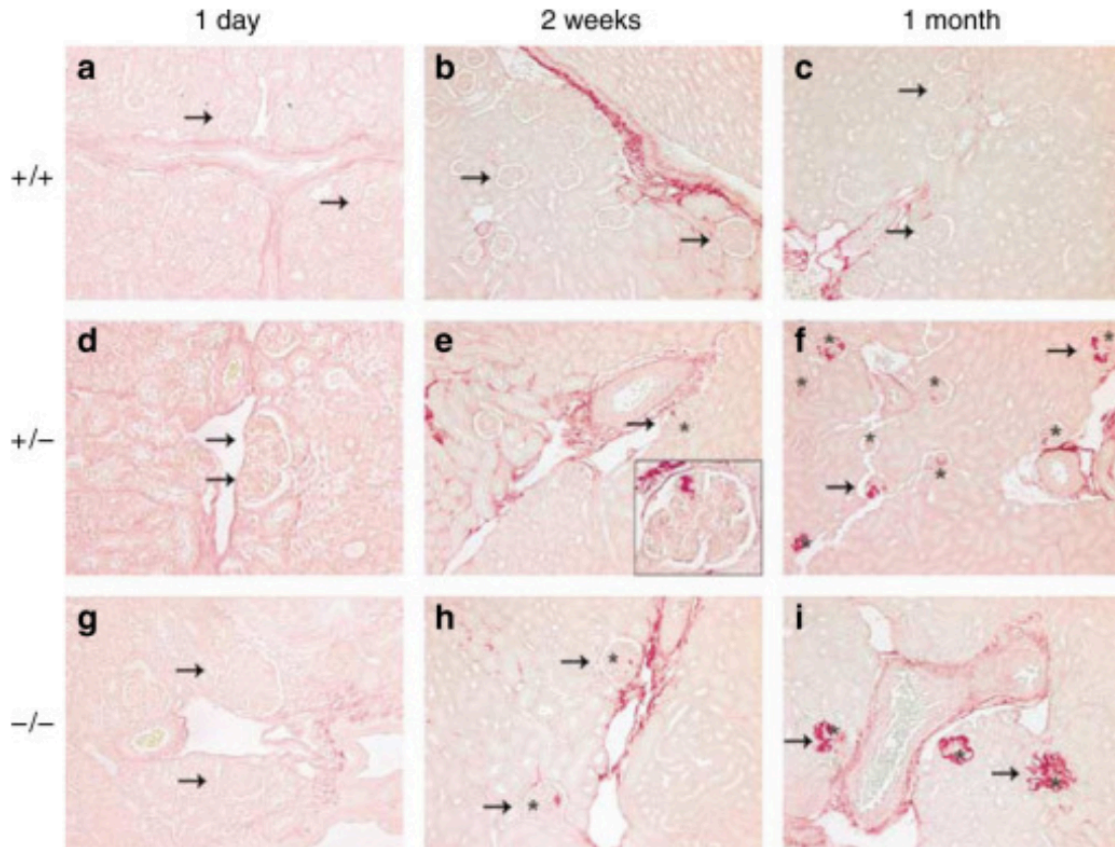


Figure 6. Initiation of type I collagen deposition in glomeruli occurs postnatally. Picosirius red stain of (a, d, and g) 1-day-old, (b, e, and h) 2-week-old, and (c, f, and i) 1-month-old mice. (a–c) Wild-type (+/+) mice do not demonstrate collagen deposition and have lesion scores of 0. (d–f) Heterozygous (+/-) mice show evidence of disease at 2 weeks (inset: enlargement of indicated glomeruli (e)), demonstrating lesion scores of 0 at 1 day, 1 at 2 weeks, and 1 at 1 month. (g–i) *Colla2-deficient* (-/-) mice also show evidence of deposition at 2 weeks with a lesion score of 0 at 1 day, 1 at 2 weeks, and 4 at 1 month. Arrows indicate glomeruli. Asterisks denote affected (Picosirius red+) glomeruli.⁷

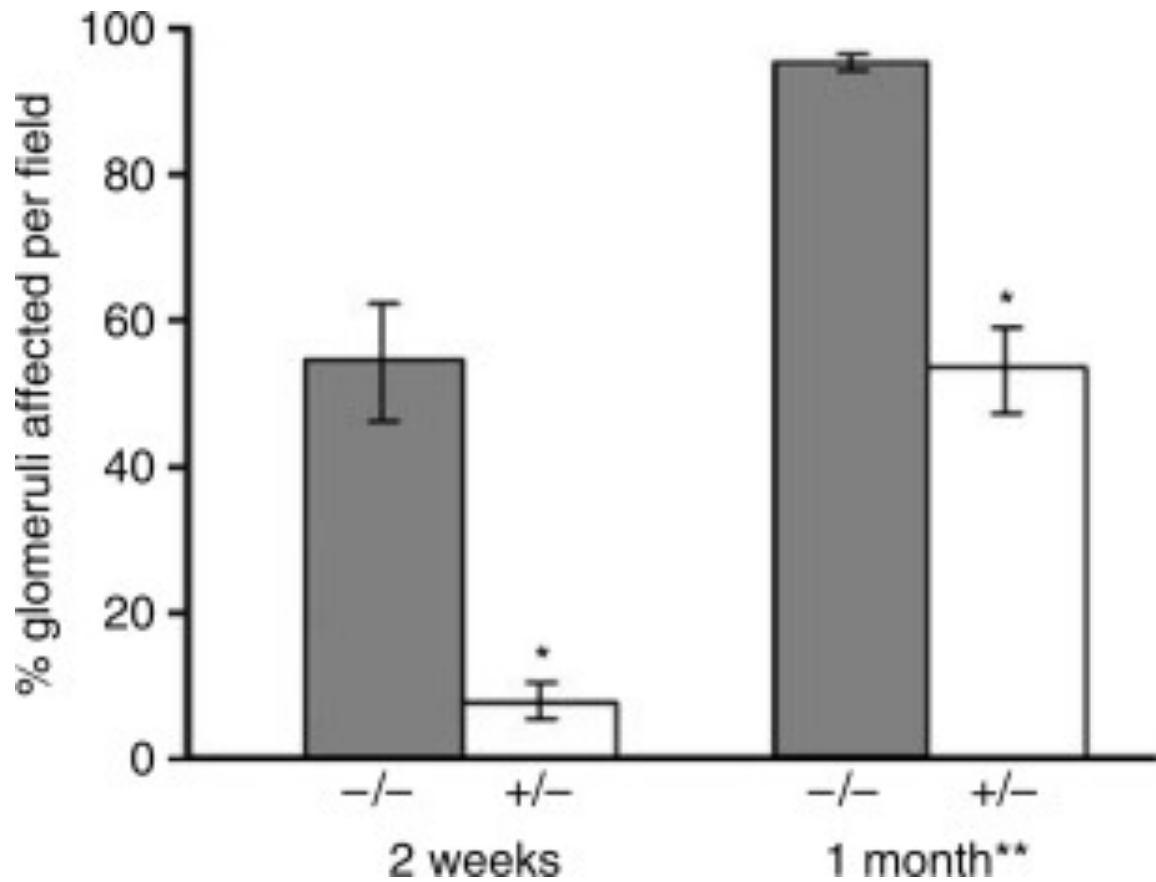


Figure 7. The type I collagen glomerulopathy in heterozygous mice demonstrate a gene dose effect (* $P < 0.0001$) that is progressive with age ($P < 0.0001$). The percent of affected glomeruli per field is significantly greater in *Colla2*-deficient (-/-) than heterozygous (+/-) kidneys at both 2 weeks and 1 month of age. Significant differences in the percent of glomeruli affected between kidneys examined at 2 weeks and 1 month of age is also shown irregardless of genotype.⁷**

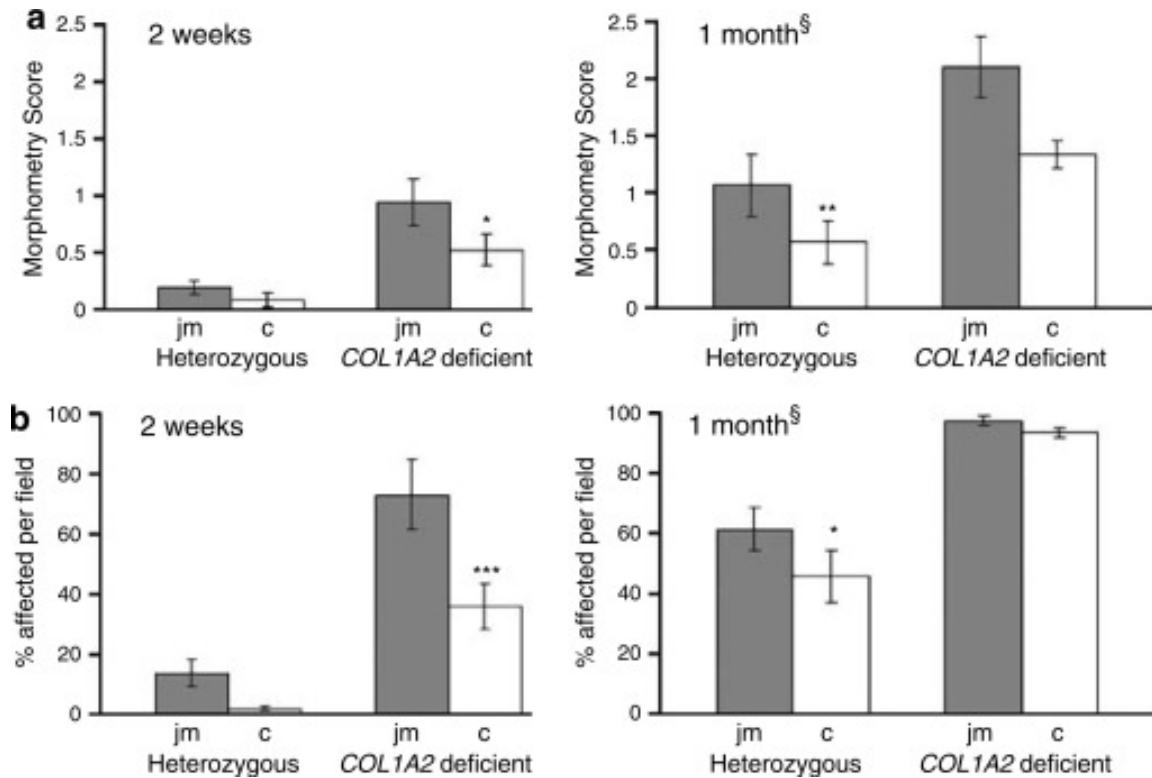


Figure 8. The type I collagen glomerulopathy initiates postnatally and glomeruli sequentially become affected in a centrifugal pattern from the juxtamedullary (jm) to the cortical (c) region in a distribution consistent with glomerular maturation and initiation of function. (a) Demonstrates that there is a significant difference between the morphometry score in jm and c glomeruli at 2 weeks and 1 month of age in *Colla2-deficient* mice with more severely affected glomeruli located in the jm region where glomerular function initiates. **(b)** Demonstrates a significant difference between percent of glomeruli affected per field between jm and c glomeruli in *Colla2-deficient* mice at 2 weeks of age whereas greater than 90% of jm and c glomeruli per field are affected by 1 month of age. Conversely, the heterozygous animals lack a significant difference at the earlier time point but demonstrate a significant difference in both lesion severity and percent glomeruli affected per field between jm and c glomeruli at 1 month of age. Further, the lesion severity and percent glomeruli affected is significantly different between the 2 week and 1 month ages (§), confirming the progressive nature of the glomerulopathy (* $P < 0.05$, ** $P < 0.005$, *** $P < 0.0001$).⁷.

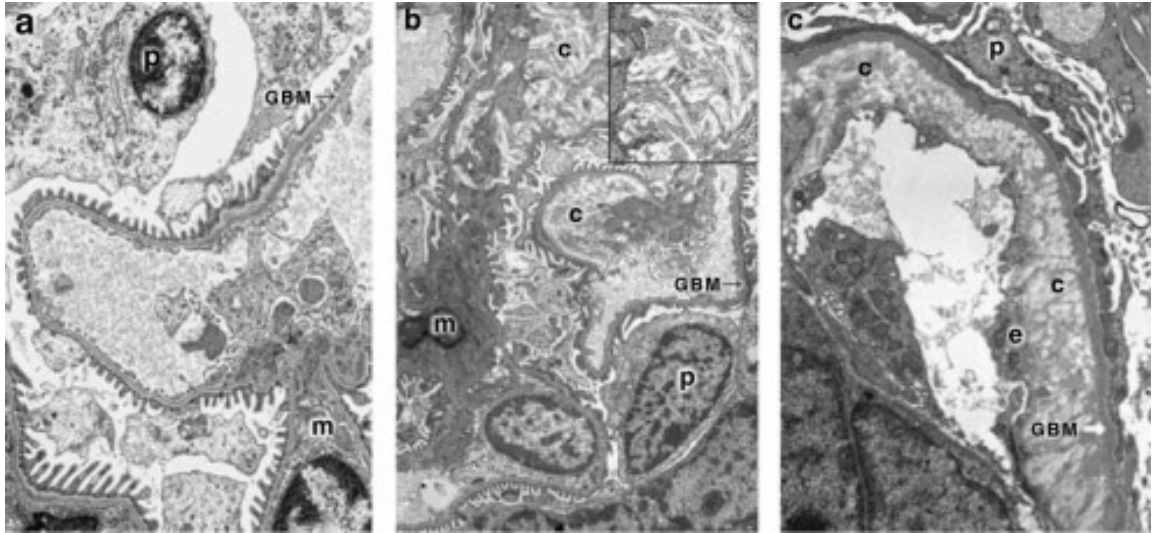


Figure 9. Electron Microscopy of Glomeruli from Wild Type and *Colla2*-deficient Mice. (a) Electron microscopy of glomeruli from wild-type and (b and c) *Colla2*-deficient mice (lesion score 4) demonstrate that the *Colla2*-deficient glomeruli exhibit deposition of extracellular fibrillar type I collagen (c) into the subendothelial space displacing the fenestrated endothelium (e) from the underlying glomerular basement membrane (b). Fibrils demonstrating cross striation of organized collagen (b; inset) were also present. In areas of severe collagen deposition and expansion of the subendothelial space, podocyte (p) foot process effacement is seen (c). It is hypothesized that the type I collagen is being produced by the mesangial (m) cell followed by deposition in the subendothelial space. In all mice examined, the glomerular basement membrane (GBM) was intact. Wild-type provided for comparison (a).⁷

Table 1. *Col1a2*-deficient mice demonstrate albuminuria in comparison to wild type animals.⁷

Genotype	n	Albumin (μg)/creatinine (mg)(range)
Wild-type	12	0.50 \pm 0.14 (0.06-1.43)
<i>Col1a2</i> -deficient	14	38.19 \pm 12.33* (0.41-128.55)
<i>Lesion Score</i>		
0	12	0.50 \pm 0.14
1	1	0.41
2	4	8.91 \pm 6.53**
3	6	42.27 \pm 20.63*
4	3	81.65 \pm 25.15*

** P<0.0001

* P<0.005

found to be the primary mechanism of type I collagen glomerulopathy. Therefore, it is suggested that a decrease in degradation of collagen may be the cause type I collagen glomerulopathy.

Deficiency in the degradation of homotrimeric type I collagen in the *Colla2-deficient* may be leading to the deposition. Matrix metalloproteinases (MMPs) are responsible for the regulation of the ECM, thereby, the degradation of collagen accumulation. MMP 2, 3, 9, and 13 are expressed in the kidney and have the ability to cleave type I collagen. There was an upregulation of mRNA for MMP 2,3, and 9 at three months of age in *Colla2-deficient* mice and there was no change in that of the heterozygous mice (Figure 12. A-C). MMP 13 is responsible for targeting and cleaving the $\alpha 2(I)$ chain and was not elevated in the *Colla2-deficient* mouse model.¹⁴

It was further shown that MMP 2 and MMP 3 were both elevated at one month for the *Colla2-deficient* mice (Figure 12. D&E).¹⁴ In order for MMPs to be responsible for this event, mRNA would have to increase before an increase in collagen deposition, however, this was not seen. It was concluded that MMPs were not the primary event leading to the pathology of homotrimeric type I collagen deposition in this model.¹⁴

Therefore, MMPs may play a role in the pathology of the *Colla2-deficient* mouse model but are not the primary mediator of homotrimeric type I collagen deposition.

Investigation into what initiates the type I collagen deposition was then pursued.

Investigation into the Potential Role of TGF- β in *Colla2-deficient* Mice

The renal mesangium comprises greater than 30% of the total glomerulus. In this location mesangial cells reside and are mediators of the wound healing response. In

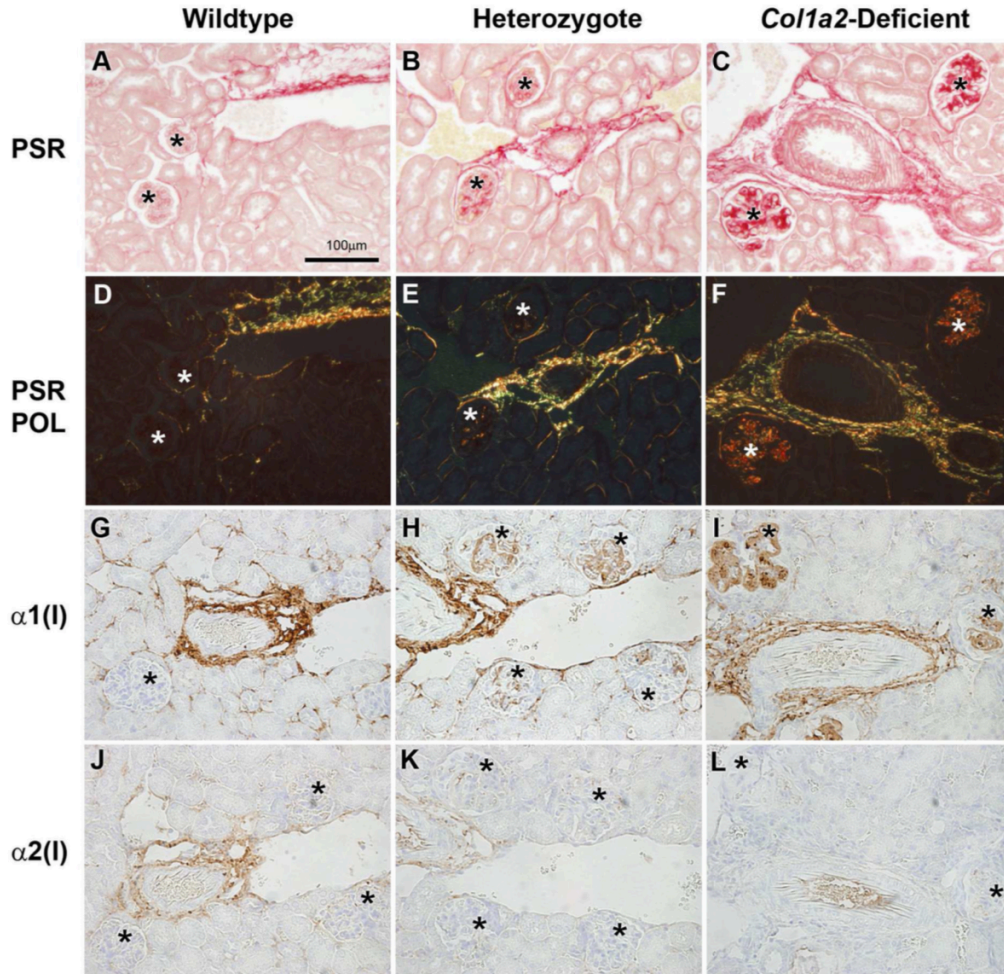


Figure 10. Identification of type I collagen homotrimer in wildtype (+/+) (A,D,G,J), heterozygous (+/-) (B,E,H,K) and homozygous (-/-)(C,F,I,L) glomeruli. Picosirius red (PSR) staining under normal (A,B,C) and polarized light (D,E,F) of wildtype glomeruli (A,D) show no deposition of type I collagen, heterozygous glomeruli (B,E) show mild deposition of type I collagen, and homozygous glomeruli (C,F) show severe deposition of collagen within glomeruli. Anti- $\alpha 1(I)$ collagen immunohistochemistry (IHC)(G–I) of wildtype kidneys (G) demonstrate no localization of $\alpha 1(I)$ chains within glomeruli, only in the vasculature. Heterozygous kidneys (H) show localization of type I collagen $\alpha 1(I)$ chains within the glomeruli and vasculature. Homozygous kidneys (I) mice also show evidence of type I collagen $\alpha 1(I)$ in the glomeruli and vasculature. Anti- $\alpha 2(I)$ collagen IHC (J–L) of wildtype (J), heterozygous (K), and homozygous (L) kidneys demonstrate the presence of $\alpha 2(I)$ chains in the vasculature of wildtype and heterozygous kidneys, and the absence of anti- $\alpha 2(I)$ positive staining within glomeruli of wildtype, heterozygous, and homozygous kidneys. Asterisks indicate glomeruli.¹⁴

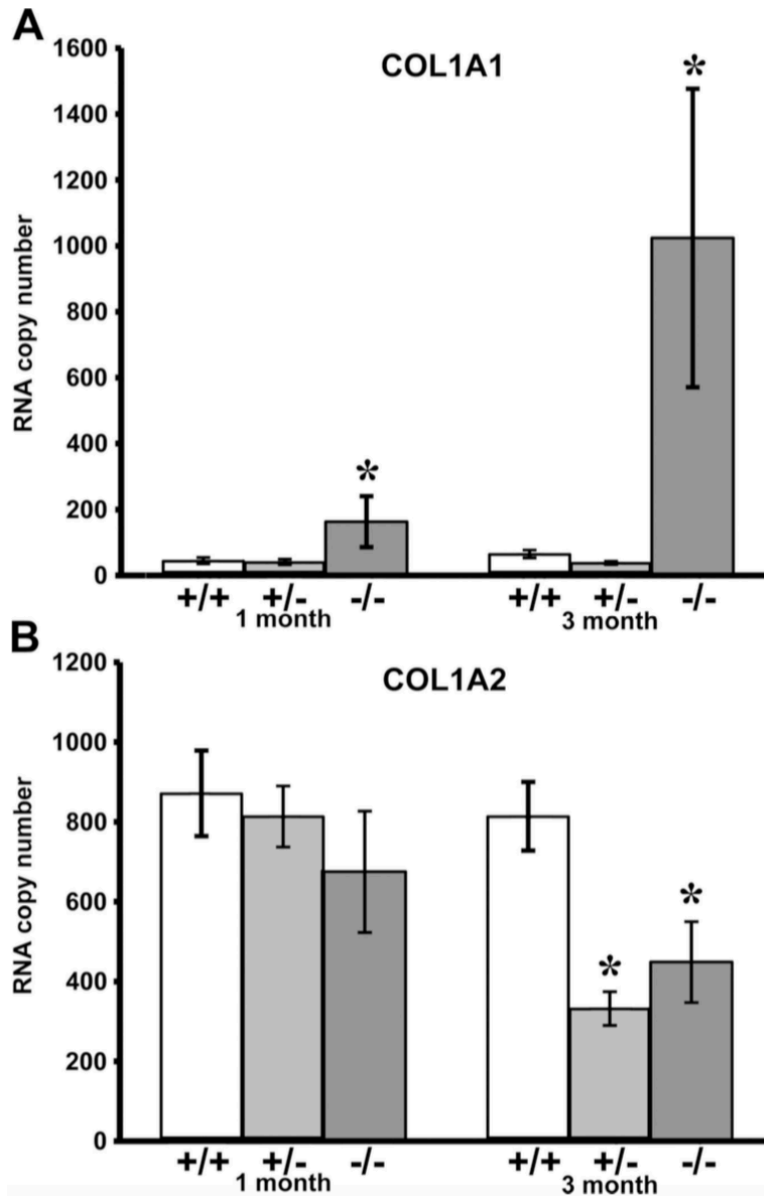


Figure 11. Quantitative RT-PCR steady-state mRNA expression. COL1A1 (top) and COL1A2 (bottom) transcripts in wildtype (+/+), heterozygous (+/-) and homozygous (-/-) *Col1a2*-deficient glomeruli. 1-month and 3-month old homozygous glomeruli demonstrate increases in pro α 1(I) collagen mRNA copy as compared to age-matched wildtype and heterozygous glomeruli (* $p < 0.003$ and * $p < 0.0001$ respectively). Pro α 2(I) collagen mRNA copy number decreases in 3-month old heterozygous (* $p < 0.0001$) and homozygous (* $p < 0.003$) glomeruli as compared to age-matched wildtype glomeruli.¹⁴

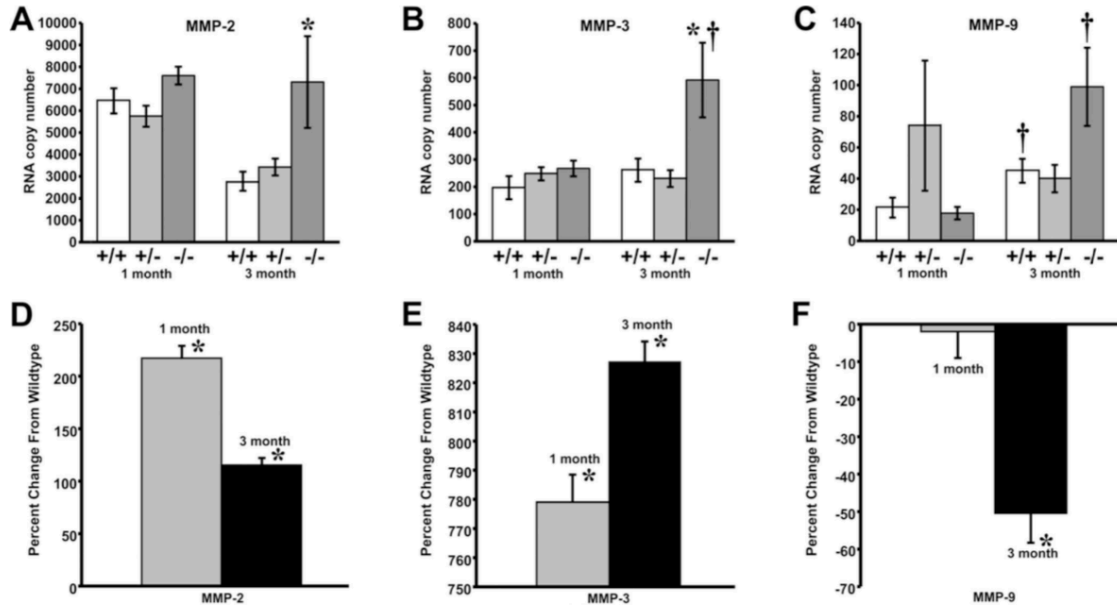


Figure 12. MMP-2, -3, and -9 Quantitative RT-PCR. Demonstrates an increase in MMP-2 (A), and MMP-3 (B) mRNA expression in 3-month *Colla2*-deficient ($-/-$) glomeruli compared to age-matched wildtype ($+/+$) [MMP-2, $*p < 0.0004$; MMP-3, $*p < 0.04$]. MMP-3 (B) and MMP-9 (C) demonstrate significant increases between 1-month and 3-month wildtype and *Colla2*-deficient glomeruli [MMP-3, $\dagger p < 0.04$ *Colla2*-deficient glomeruli; MMP-9, $\dagger p < 0.01$ wildtype and MMP-9, $\dagger p < 0.0007$ *Colla2*-deficient glomeruli]. 1-month and 3-month *Colla2*-deficient glomeruli show an increase in MMP-2 (D) ($*p \leq 0.001$ and $*p \leq 0.008$ respectively), and MMP-3 (E) ($*p \leq 0.0005$ and $*p \leq 0.0003$ respectively) protein expression as compared to age-matched wildtype mice, while MMP-9 (F) shows a decrease in protein expression at three months of age ($*p \leq 0.05$). Data expressed as mean \pm SEM.¹⁴

addition, mesangial cells are capable of producing type I collagen in response to damage.³⁰ Collagen deposition and renal injury has been shown to occur at one week of age in the *Colla2-deficient* mouse model.⁷ Transforming growth factor- β 1 (TGF- β 1) was first studied to see if it is responsible in mediating this deposition. TGF- β 1 has been found to be upregulated in models of liver and kidney fibrosis. The effects of this upregulation resulted in serum increases of this growth factor, as well as, increased collagen deposition in the subendothelial space.^{31,32} It had previously been discovered that TGF- β 1 is released by mesangial cells under specific conditions.³³ It has also been shown to activate/stimulate mesangial cells.³⁴ Upon activation these mesangial cells can then differentiate into cells that exhibit myofibroblast-like phenotypes.^{35,36} TGF- β 1 is also suggested that TGF- β 1 is capable of activating myfibroblastic cells³⁷⁻⁴⁰, the result of which, is an increase in ECM accumulation and production. Matrix metalloproteinases (MMPs) play a critical role in this progression, as they have been shown to activate TGF- β 1.^{34,41} This activation is correlated to TGF- β 1 inducing epithelial-mesenchymal-transition (EMT) in multiple types of cancers: lungs, kidneys, liver, and prostate.^{42,43}

EMT has been described as the loss of intercellular junctions, detachment of the epithelium from the basement membrane, a decrease in epithelial protein markers, and an increase of mesenchymal markers. Due to the increase in mesenchymal phenotype these cells have the ability to traverse the basement membrane and differentiate into multiple cell types. TGF- β 1 is capable of inducing EMT in different renal fibrosis models through a range of mediators.⁴⁴ Markers of EMT are vimentin, desmin, and α -SMA.⁴⁵ The presence of myofibroblasts indicate that EMT could be occurring. Myofibroblasts have the ability to contract and play a role in the wound healing response/process.⁴⁴ The

process by which myofibroblasts are found in the renal mesangium has yet to be shown but three postulations have been made. First, that myofibroblasts arise from differentiation of epithelial cells in the renal interstitium and traverse the Bowman's capsule through breaks from previous damage. Second, is that myofibroblasts are formed from mesangial cells due to the over expression of α -SMA triggering EMT. Third, is that myofibroblasts arise from epithelial cells that make up the Bowman's capsule itself and when this happens the capsule begins to break down, thereby, releasing myofibroblasts into the glomerular mesangium.⁴⁶

It has been previously shown that proximal tubule cells undergo EMT and begin expressing α -SMA when signaled by TGF- β . Additionally, the cytoskeleton around these cells reorganizes into longitudinal bundles of fibers, which are referred to as stress fibers. α -SMA gets incorporated into these stress fibers firmly securing the cell to the extracellular matrix. Stress fibers are a characteristic associated with myofibroblast formation and are used as an indicator for EMT.^{47,48}

A study done in 2002 explored mesenchymal markers, their expression, and collagen deposition in 133 biopsies from patients with renal disease. The study found that the basement membrane, when intact, showed expression of vimentin in the tubular cells, but not all tubular cells expressed α -SMA. For collagen, both type I and type III were present in the tubular cells. Interstitial fibrosis and the number of tubular cells that exhibited markers of EMT were directly related, and this was further shown to be in direct correlation patient's creatinine levels.⁴⁹

Due to the findings of these studies and the potential role of TGF- β 1 inducing EMT it was postulated that TGF- β 1 could be playing a role in activating EMT in the

Colla2-deficient mouse model leading to the deposition of homotrimeric type I collagen in the renal mesangium. *Colla2-deficient* mice were analyzed for presence and localization of vimentin, desmin, α -SMA, and PCNA (Proliferating Cell Nuclear Antigen) via IHC (Figure 13). PCNA is involved in proliferation of cells through its localization to the nucleus where it is critical for DNA replication, however, upon cell damage PCNA is ubiquitinated for degradation.⁵⁰ Proliferation was evaluated through PCNA labeling. Vimentin, desmin, and α -SMA were present and had a greater labeling in the parietal epithelium of glomeruli of *Colla2-deficient* mice (Figure 13 B&D, F&H, J&L). The localization of these markers suggested that EMT was in fact occurring. The localization and labeling of PCNA decreased in *Colla2-deficient* mice, which could indicate cell death or damage and a decrease in proliferation of mesangial cells (Figure 13 N&P). It could also be speculated that these cells are being displaced due to the deposition of homotrimeric type I collagen in the renal mesangium and, are therefore, being pushed to the periphery.⁵¹

mRNA and protein levels of TGF- β 1 were not increased in *Colla2-deficient* as compared to wild type at one-month or three-months of age. Interestingly, TGF- β 1 mRNA was actually reduced in *Colla2-deficient* mice (Figure 14A). TGF- β 1 protein was not localized within the glomeruli of frozen or paraffin-embedded kidneys from wild type, heterozygote, or *Colla2-deficient* mice at one-month or three-months of age when evaluated via IHC (Figure 14B).⁵¹

Therefore, it was concluded that TGF- β 1/Smad3 was uninvolved in the early stages of the disease through the comparison of scoring of *Colla2-deficient* mice with *Colla2-deficient/Smad3-deficient* knockout mice at one-week of age. The absence of

TGF- β 1 via Smad3 signaling did not affect severity of the disease (Figure 15). It is suggested that TGF- β 1 signaling via Smad3 is not the primary initiator of homotrimeric type I collagen deposition in the *Colla2-deficient* model.⁵¹

Investigation into the Potential Role of TNF- α in *Colla2-deficient* Mice

Another signaling pathway with a potential role in collagen accumulation in *Colla2-deficient* mice is tumor necrosis factor- α (TNF- α). TNF- α is a known inflammatory cytokine that responds to damage or injury in tissue. Mesangial cells have been shown to also release TNF- α upon exposure to various pathogens.⁵² Mesangial-derived TNF- α has been suggested to be responsible for podocyte effacement. Effacement of podocytes leads to proteinuria⁵³ and complete podocyte loss.⁵⁴ EMT in multiple cancer types has also been shown to result from TNF- α signaling, including renal cell carcinoma.⁵⁵ TNF- α has also been shown to increase in plasma and urine of individuals with diabetic nephropathy⁵⁶ and primary nephrotic syndrome.⁵⁷ Due to EMT and mesangial cell proliferation caused by TNF- α it was hypothesized that TNF- α may be responsible for homotrimeric type I collagen deposition in the *Colla2-deficient* mouse model.

The role of TNF- α was evaluated through the use of a known TNF- α inhibitor, Etanercept. Etanercept is a fusion protein comprised of soluble TNF- α receptor (sTNF- α receptor), and IgG antibody. The fusion acts as a competitive inhibitor of TNF- α . Etanercept has a half-life five times longer than the endogenous sTNF- α receptor and has an affinity for TNF- α 50-fold higher than the endogenous receptor. The result of this is enhanced ability to bind TNF- α , thereby, reducing the pathogenic effects and improving

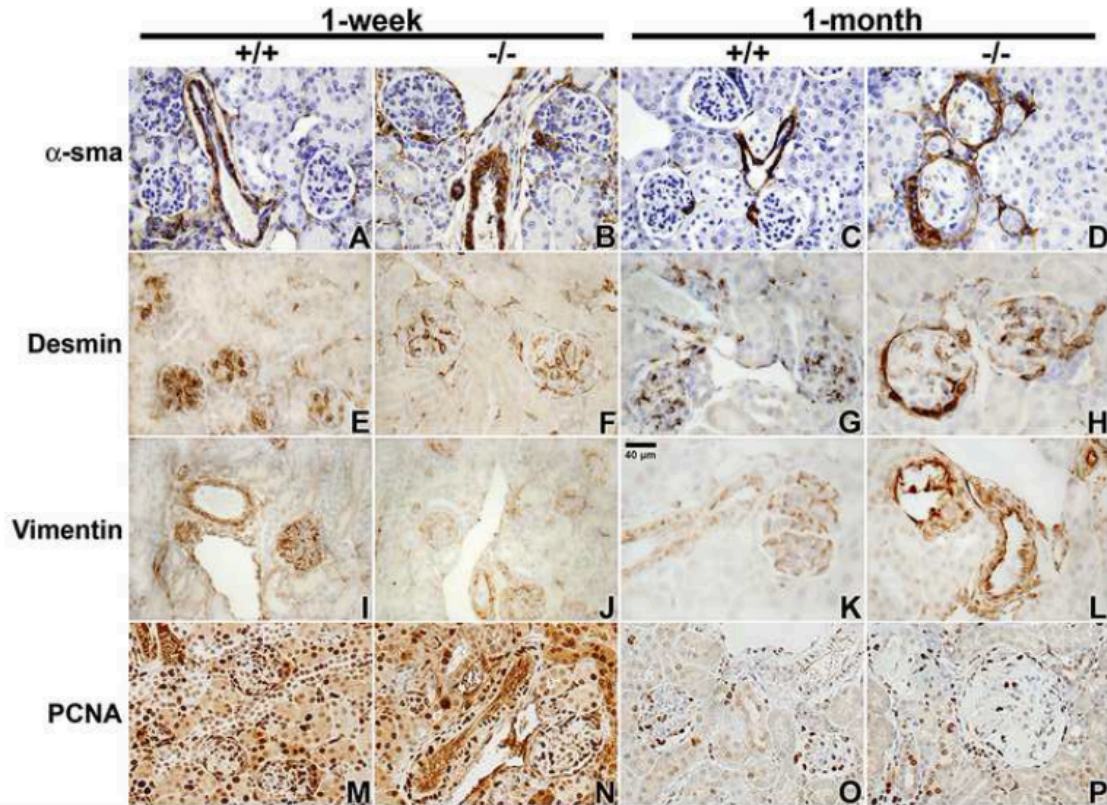


Figure 13. *Colla2*-deficient (-/-) glomeruli demonstrate parietal epithelial cell (PEC) EMT at 1-month of age. Immunostaining of 1-week and 1-month +/+ and -/- kidneys with α -sma, Desmin, Vimentin, and PCNA. Immunostaining at 1-week of age demonstrates glomerular α -sma (A, B), desmin (E, F), vimentin (I, J), and PCNA (M, N) in both +/+ and -/- within the same regions, consistent with developmental expression. α -sma is seen in the vascular pole of +/+ glomeruli (C); in contrast to -/- glomeruli (D), which show α -sma staining in PECs and in the mesangium. At 1-month of age, +/+ kidneys demonstrate desmin (G) and vimentin (K) staining in podocytes while -/- glomeruli demonstrate intense desmin (H) and vimentin (L) staining in PECs and a redistribution of positive staining in podocytes to the periphery. PCNA positive staining was seen in +/+ (O) and -/- (P) glomeruli at 1-month of age; however, there was a decrease in intraglomerular staining and an increase in PEC positivity as compared to +/+ glomeruli.⁵¹

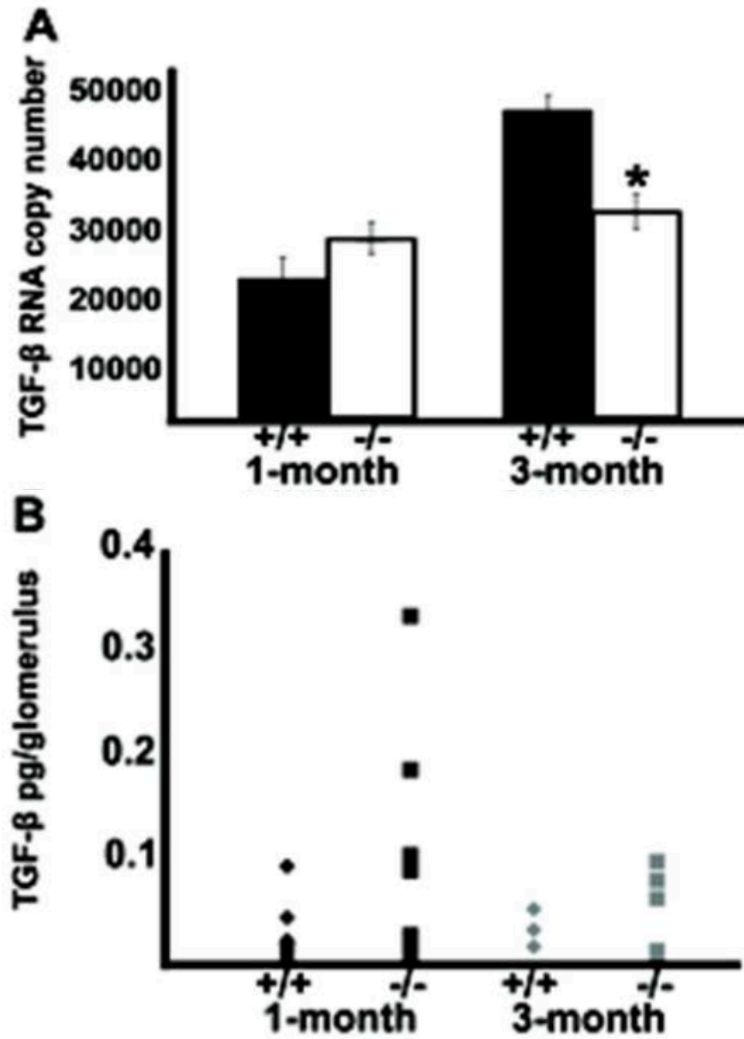
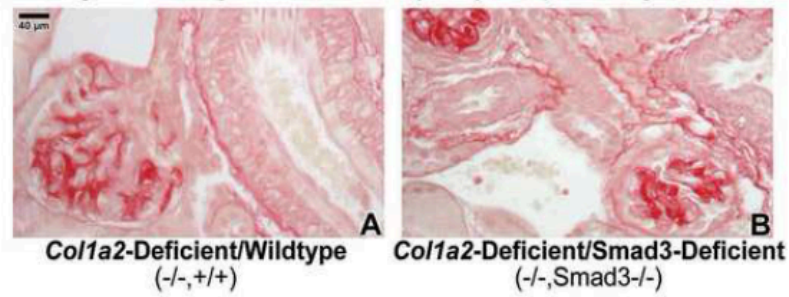


Figure 14. TGF- β 1 steady-state mRNA and protein are not upregulated in homotrimeric type I collagen glomerulopathy. (A) Quantitative RT-PCR demonstrates that TGF- β 1 copy number is not significantly different in glomerular isolates of 1-month old wildtype (+/+) and *Colla2-deficient* (-/-) mice. However, by 3-months of age TGF- β 1 copy number is elevated in wildtype glomerular isolates compared to 1-month +/+ and 1- and 3-months of age *Colla2-deficient* glomerular isolates. (B) Although protein immunoassay demonstrated no significant difference in picograms (pg) of TGF- β 1 protein per glomerulus in wildtype (+/+) and *Colla2-deficient* (-/-) glomeruli at both 1-month and 3-month of age, *Colla2-deficient* (-/-) glomeruli at 1-month of age exhibited a greater variability in TGF- β 1 protein per glomerulus.⁵¹



	Wildtype (+/+)	Heterozygous (+/-)	Col1a2-Deficient (-/-)
Wildtype (+/+)	0 (+/+, +/+)	2.29 ± 0.30 (+/-, +/+)	3.50 ± 0.33 (-/-, +/+)
Smad3-Deficient (+/-)	0 (+/+, Smad3 ^{+/-})	2.21 ± 0.21 (+/-, Smad3 ^{+/-})	3.50 ± 0.19 (-/-, Smad3 ^{+/-})
Smad3-Deficient (-/-)	0 (+/+, Smad3 ^{-/-})	1.90 ± 0.25 (+/-, Smad3 ^{-/-})	3.22 ± 0.27 (-/-, Smad3 ^{-/-})

Figure 15. *Col1a2*-deficient/*Smad3*-deficient glomeruli demonstrate homotrimeric type I collagen deposition. (A) 1-month *Col1a2*-deficient glomerulus demonstrating fibrillar collagen deposition upon staining with picrosirius red. (B) 1-month *Smad3*-deficient glomeruli demonstrating similar intensity of picrosirius red staining. Mean lesions scores for 1-month *Col1a2*-deficient/*Smad3*-deficient animals are provided in the table (below) and demonstrate no significant differences.⁵¹

symptoms of affected individuals.⁵⁸

Investigation into the Potential Role of PDGF in *Colla2*-deficient Mice

Platelet derived growth factor (PDGF) has been shown to be upregulated in most renal diseases, play a role in mesangial proliferation and interstitial proliferation, and be upregulated in response to renal injury/damage.⁵⁹ PDGF ligands and receptors also play a role in myofibroblast proliferation, collagen production, and promotion of cell adhesion. These same ligands/receptors are regulated through ECM proteins and glycoproteins, both of which are increased throughout the progression of fibrosis.⁶⁰

Five hetero/homo-dimeric proteins, PDGF-AA, PDGF-BB, PDGF-AB, PDGF-CC, and PDGF-DD classify the ligands of PDGF. There are three tyrosine kinase receptors that these ligands interact with, PDGFR- $\alpha\alpha$, PDGFR- $\beta\beta$, and the less characterized PDGFR- $\alpha\beta$ (Figure 16).⁶¹ PDGF-AA and -BB were the first to be discovered^{59,62,63} with PDGF-CC and -DD being discovered later. PDGF-AA and -BB are different than -CC and -DD, in that, PDGF-CC and -DD are secreted with an N-terminal domain, known as a CUB (complement C1r/C1s, Uegf, Bmp1) domain. This domain must be cleaved in order for the ligands to interact with their corresponding receptor.^{59,64} Auto phosphorylation occurs upon binding of ligands to their receptors, causing dimerization of the receptors and downstream signaling.⁶¹

The pathways affected by PDGF ligands and their receptors include, but are not limited to, rat sarcoma-mitogen-activated protein kinase (Ras-MAPK), phospholipase C- γ (PLC- γ), and phosphatidylinositol-3-kinase (PI3K) (Figure 16). PDGF ligands and receptors have been shown to play critical roles in the development of renal tissue in mice.⁶¹ Ras-MAPK is highly conserved across species and has been shown to play a role

in cellular proliferation, metabolism, differentiation, motility, apoptosis, and survival. In addition, this signaling cascade is very complex and inducible through multiple different mediators.⁶⁵ PLC- γ is less characterized than Ras-MAPK, however, PLC- γ has been shown *in vivo* to play a role in the development of the kidney.⁶⁶ PI3K signals Akt/PKB, a serine/threonine kinase. This pathway controls cell growth, proliferation, differentiation, and survival, which is speculated to play a critical role in the development of fibrosis in kidney disease.⁶⁷

Early in mouse renal development, PDGF-AA, -BB, -CC, and -DD are expressed.⁵⁹ Knockout mice have been studied in great detail and have demonstrated the imperative role of PDGF in the development of mice. Knockouts of PDGF-AA, -BB, -CC, PDGFR- $\beta\beta$, and - $\alpha\alpha$, die prenatally or just after birth.^{59,68} PDGFR- $\alpha\alpha$ knockouts show a deficit in the renal mesenchyme, the consequences of which are abnormal nephron development.⁶⁹ Knockouts of PDGF-BB and its corresponding PDGFR- $\beta\beta$ result in malformation of the capillary tuft or capillary loops due to the lack of mesangial cells that provide the structural scaffolding for capillaries. This results in an increase in diameter of capillaries and a decrease in capillary organization. Mesangial cells are critical for the organization, filtration efficiency, and surface area of glomerular capillaries.⁷⁰⁻⁷²

The role of these ligands and receptors have been implicated in various forms of disease pathways, including fibrosis and cancers. Smooth muscle cells and fibroblasts respond to PDGF, leading to fibrosis and scarring in the lungs, liver, kidney, skin, and heart.⁷³ Chronic glomerulosclerosis has been shown to be driven by PDGF-BB and -DD resulting in secondary tubulointerstitial fibrosis (TIF). It has been further shown that

PDGF-DD has profibrotic outcomes on the tubular interstitium through the potential of EMT. In glomeruli, mesangial cell proliferation has been shown to be induced through the over production of PDGF-BB and -DD ligands via PDGFR- $\beta\beta$.^{74,75} Taken together these effects indicate that PDGF is a key regulator of mechanisms that lead to fibrotic and proliferative abnormalities in the kidney, more specifically, in the glomeruli of the nephrons. A PDGF-DD knockout has yet to be characterized.⁶¹

PDGFR- $\alpha\alpha$ is expressed in the renal interstitium, smooth muscle cells, and mesangial cells. Mesangial, parietal epithelial, and interstitial cells all express PDGFR- $\beta\beta$, as well as, smooth muscle cells of the renal arteries. PDGF-AA has been observed in epithelial cells and mature podocytes. The expression of PDGF-BB has for the most part been hard to confirm via IHC, however, it has been shown in low levels within the renal mesangium expressed by mesangial cells.⁷⁶ Finally, in mice PDGF-DD has been expressed, exclusively, by mesangial cells.^{61,77}

In fibrotic models, especially in mice, it has been shown that the expression of PDGFs, ligands and receptors, are upregulated.⁵⁹ PDGF-CC has been shown to be expressed in TIF areas on infiltrating macrophages and interstitial cells.^{76,78} PDGF-BB has been widely studied and has been shown to be expressed on a wide variety of cells in fibrotic models.⁵⁹ Most importantly for our model, PDGF-BB is expressed in mesangial cells and podocytes.⁵⁹ PDGF-DD has been least characterized out of the PDGF ligands.⁶¹ Finally, PDGFR- $\beta\beta$ is shown to be over expressed in fibrotic areas within the renal mesangium and endothelial cells.⁵⁹

Recent research has been done to assess the regulation via fucosylation of PDGFR- $\beta\beta$ and TGF- β 1 receptor through an enzyme fucosyltransferase (FUT). While

there are multiple FUTs, FUT8 was studied as it is responsible for the regulatory mechanism of these two receptors. FUT8 knockdown (siRNA and shRNA) reduced the prevalence of α -SMA in both PDGFR- $\beta\beta$ and TGF- β 1 receptor.⁷⁹ This result could have implications for the *Colla2-deficient* mouse model and homotrimeric type I collagen glomerulopathy.

Aims

The first aim of this study was to examine the effect of a TNF- α inhibitor in the *Colla2-deficient* mouse model using Etanercept, a known TNF- α inhibitor. The second aim of this study was to determine if there is differential labeling, via IHC, of PDGF-BB, PDGF-DD, and PDGFR- $\beta\beta$ in the *Colla2-deficient* mouse model in comparison to the wild type mice.

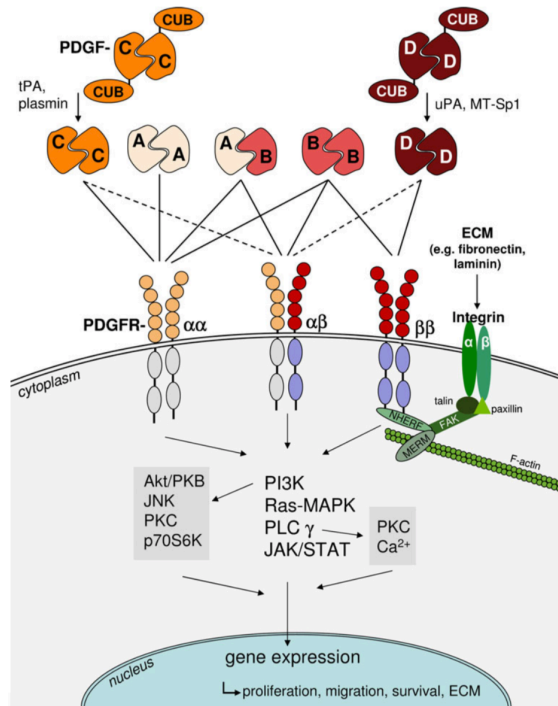


Figure 16. Simplification of main molecules involved in PDGF-PDGFR interactions.

PDGF -AA, -AB, and -BB are secreted in an active form whereas PDGF -CC and -DD have to be proteolytically cleaved to allow binding of the ligands to their receptors. Proteases known to split off the PDGF-CUB domains are tPA or plasmin (PDGF-CC), and uPA or MT-Sp1 (PDGF-DD). PDGF binding results in autophosphorylation of the cytoplasmic tyrosine kinase domain of the PDGF receptor chains and subsequently recruits adaptor proteins carrying Src homology 2 (SH2) and SH3 domains to this site. Downstream signaling occurs mainly via the JAK/STAT, PI3K, PLC- γ , or RAS-MAPK pathways, promoting gene expression and mediating the biological functions of the PDGF isoforms, e.g. proliferation, migration, and survival. A highly relevant profibrotic crosstalk is the cooperation of PDGF and integrin signaling. NHERFs were shown to link PDGFR- β with focal adhesion kinase and the cortical actin cytoskeleton, thereby enhancing PDGF-induced MAPK signaling. For simplification of the scheme, many other regulatory processes, e.g., processes limiting the PDGF response, are not included but are mentioned in the text. Also, not shown are transactivation processes of PDGFRs without ligand binding by, e.g., G-protein-coupled receptors. PDGF, platelet-derived growth factor, PDGFR PDGF receptor, CUB complement C1r/C1s, Uegf, Bmp1, tPA tissue-type plasminogen activator, uPA urokinase-type plasminogen activator, MT-Sp1 matrilysin, ECM extracellular matrix, NHERF Na⁺/H⁺ exchanger regulatory factor, MERM merlin and ezrin/radixin/moesin family of cytoskeletal linkers, FAK focal adhesion kinase, JAK Janus kinase, STAT signal transducers and activators of transcription, PLC- γ phospholipase C- γ , PI3K phosphatidylinositol-3-kinase, JNK c-Jun amino-terminal kinase, RAS rat sarcoma, MAPK mitogen-activated protein kinase, Akt/PKB protein kinase B, PKC protein kinase C, p70S6K ribosomal protein S6 kinase beta-1.⁶¹

MATERIALS & METHODS

Picro Sirius Red (PSR) Staining

Paraffin embedded formalin fixed kidneys were sectioned at 5 microns. Picro Sirius Red (PSR) stains for fibrillary collagen and the kit for this protocol was ordered from Polysciences Inc. (Cat # 24901). The recommended procedure was followed. Sections were deparaffinized in xylene in increments of 3 minutes for three separate washes. Sections were then placed in graded ethanol washes, starting at 100% three times for three minutes. Each section was then set in 95% ethanol for 1 minute, then set in 70% ethanol for one minute. The purpose of the graded ethanol washes is to rehydrate tissue. Tissue sections were rinsed with distilled water for three minutes to prepare for staining. Samples were placed in Solution A (Phosphomolybdic acid) for two minutes. This was followed by a distilled water rinse before being placed in Solution B (Picrosirius red F3BA stain) for 60 minutes. Solution C (0.1 N Hydrochloride acid) is the next solution the tissue sections were set into for two minutes. The sections then go through graded ethanol washes to dehydrate and prepare for mounting. This procedure started with 45 seconds in 75% ethanol, followed by a one-minute wash in 95% ethanol, and finally placed in 100% ethanol for three minutes. Lastly, Permount is applied to the slides so that cover slips can be added. Slides were left to dry overnight and were visualized the next day via light microscopy.

Tissue and Histology (TNF- α)

The following mice were cared for according to protocol at the University Of Connecticut. The mice were injected intravenously with saline or Etanercept (5ug/g

bodyweight) twice weekly for 6 weeks, then sacrificed just over a week after the final dose. Kidneys from male and female wildtype and *Colla2-deficient* mice were used and divided into four previous determined categories: wildtype mice treated with the vehicle (IgG1), wildtype mice treated with Etanercept (a TNF- α inhibitor), *Colla2-deficient* mice treated with vehicle, and treated *Colla2-deficient* mice using Etanercept. These kidneys were evaluated for the presence of fibrillar collagen deposition and given a lesion score (M0 through M4) to represent the severity of the deposition. Kidney blocks were received from Charlotte L. Phillips, PhD at the University of Missouri.

Tissues were prepared by IDEXX BioResearch in Columbia, MO using standard formalin fixation and paraffin embedding procedure. In all, 37 kidneys were sectioned in a longitudinal fashion measuring 7 μ m in thickness using a Leica RM2135 microtome on the Missouri State University campus. These samples were taken from seven-week old wildtype and *Colla2-deficient* mice. The sections were then mounted on positively-charged slides, labeled, and placed on a covered slide warmer for 30 minutes to dry. After, they were placed in a slide box and stored in a refrigerator at 4°C for later use.

Lesion Scoring (TNF- α)

Sections were examined via conventional light microscopy to evaluate the presence of collagen within glomeruli of *Colla2-deficient* mice in comparison to wild type mice. Lesion scoring is based on the severity of collagen that is present within glomeruli and the scoring is as follows: G0 – no lesioning, G1 – mild lesions with less than 25% of the glomeruli affected, G2 – moderate lesions with less than 50% of the glomeruli affected, G3 – moderately lesioned and affects less than 75% of the glomeruli, and G4 – severely lesioned and affects greater than 75% of the glomeruli.⁷

Morphometry Mapping

Morphometry mapping utilizes the lesion scoring system described above.

Morphometry scores are obtained by counting multiple fields (10x) of glomeruli and giving each one a lesion score. The scores are added up taking into account the total glomeruli count with its corresponding lesion score 0-4. An example equation is supplied below. $[(0x\#)+(1x\#)+(2x\#)+(3x\#)+(4x\#)] \div \text{Total number of glomeruli counted. (\#)}$ represents the number of glomeruli counted for each possible lesion score number, 0-4.⁷

Histology (PDGF)

Tissues were prepared by IDEXX BioResearch in Columbia, MO using standard formalin fixation and paraffin embedding procedure. Five wild type mice (2259, 2252, 2192, 2214, 2218) and five *Colla2-deficient* mice (2253, 2229, 2265, 2255, 2183) were chosen. These kidneys were sectioned in a longitudinal fashion measuring 5 μ m in thickness using a Leica RM2135 microtome on the Missouri State University campus. These samples were taken from six-week old wild type and *Colla2-deficient* mice. The sections were then mounted on positively-charged slides, labeled, and placed on a covered slide warmer for 30 minutes to dry. After, they were placed in a slide box and stored in a refrigerator at 4°C for later use.

Immunohistochemical (IHC) Labeling (PDGF)

Protocol, antibodies, and blocking reagent were bought and received from Santa Cruz Biotechnology. Indirect Immunoperoxidase Staining was performed per manufacturers' guidelines. Formalin-fixed, paraffin-embedded mice kidneys were used for sectioning via a microtome. Sections were cut at 5 microns. Antigen retrieval was achieved through a sodium citrate boil. This allowed for antigens to be unmasked and

ready for indirect immunoperoxidase staining. Blocking reagent(UltraCruz[®] Blocking Reagent, sc-516214) was used to mask any unwanted antigens that the primary antibody may have a low affinity for, thereby increasing the binding of the primary to the target. After blocking sections for 1-hour, primary antibodies were diluted in blocking reagent and added to sections. They were allowed to sit overnight in 4° C. In the morning secondary antibody were added, diluted in blocking reagent, for two hours. Sections were then incubated with SIGMAFAST 3,3'-Diaminobenzidine (DAB) (D4293-50SET), ordered from SIGMA Life Sciences, for 10 minutes in a dark room. Sections were dehydrated with increasing graded ethanol washes, finishing in xylene and were then counterstained with hematoxylin for nuclei staining. Permount was used to mount coverslips on the kidney section slides. Primary antibodies include: PDGF-BB (F-3) sc-365805, mouse monoclonal IgG_{2b} 200 ug/ml, PDGFR-ββ (D-6) sc-374573, mouse monoclonal IgG_{2a} 200 ug/ml, PDGF-DD (E-7) sc-137029, mouse monoclonal IgG_{2a} 200ug/ml. Primary antibodies were diluted (1:100) in UltraCruz[®] Blocking Reagent and secondary antibodies were diluted (1:50) in UltraCruz[®] Blocking Reagent. Secondary antibody was a Horse Radish Peroxidase (HRP) conjugated antibody: m-IgG_κ BP-HRP, sc-516102, HRP conjugated 200 ug/05.ml.

RESULTS

Tumor Necrosis Factor – Alpha

The first aim of this study was to examine the effect of a TNF- α inhibitor in the *Colla2-deficient* mouse model using Etanercept, a known TNF- α inhibitor. The goal of this aim was to determine if TNF- α is the primary mediating molecule in homotrimeric type I collagen glomerulopathy in the *Colla2-deficient* mouse model. Etanercept is a TNF- α inhibitor used to diminish TNF- α effects in this study. It was hypothesized that *Colla2-deficient* mice treated with Etanercept would show attenuated PSR positive staining in comparison to *Colla2-deficient* mice treated with vehicle.

Six-week-old male and female wildtype and *Colla2-deficient* mice were used to test TNF- α . The four different groups were as follows: wild type mice treated with vehicle (IgG1), wild type mice treated with Etanercept, *Colla2-deficient* mice treated with vehicle (IgG1), and finally, *Colla2-deficient* mice treated with Etanercept.

As has been shown previously, there was no homotrimeric type I collagen deposition in wild type mice treated with vehicle (IgG1) (Figure 17) or in the wild type mice treated with Etanercept (Figure 18). There was an observed uptake of PSR stain within the glomerulus of *Colla2-deficient* mice that were treated with vehicle (IgG1), as expected (Figure 19). *Colla2-deficient* mice treated with Etanercept also demonstrated PSR positive staining (Figure 20). Based on these results, it was concluded that Etanercept treatment was not eliminating fibrosis.

To determine if treatment was decreasing fibrosis in *Colla2-deficient* mice morphometry mapping⁷ was performed. Also, lesion severity was quantified among the

four groups. Mean lesion scores for all genotypes can be seen in Table 2. Mean lesion scores for wildtype mice treated with the vehicle was zero while those treated with Etanercept was 0.046 ± 0.038 . The mean lesion score for *Colla2-deficient* mice that were treated with the vehicle was 3.197 ± 0.191 , indicating on average, glomeruli were more than 50% filled with collagen. The mean lesion score for *Colla2-deficient* mice treated with Etanercept was 2.799 ± 0.170 , this also indicated that on average, glomeruli were greater than 50% collagenated with mild lesioning. The mean lesion score difference between the *Colla2-deficient* groups was 0.398 ± 0.256 with a p-value of 0.432. There is not a statistically significant difference in lesion scoring severity between *Colla2-deficient* mice who received the vehicle and in those who received the treatment.⁸⁰ These results indicated that TNF- α is not the primary mediating molecule in homotrimeric type I collagen glomerulopathy in *Colla2-deficient* mice.

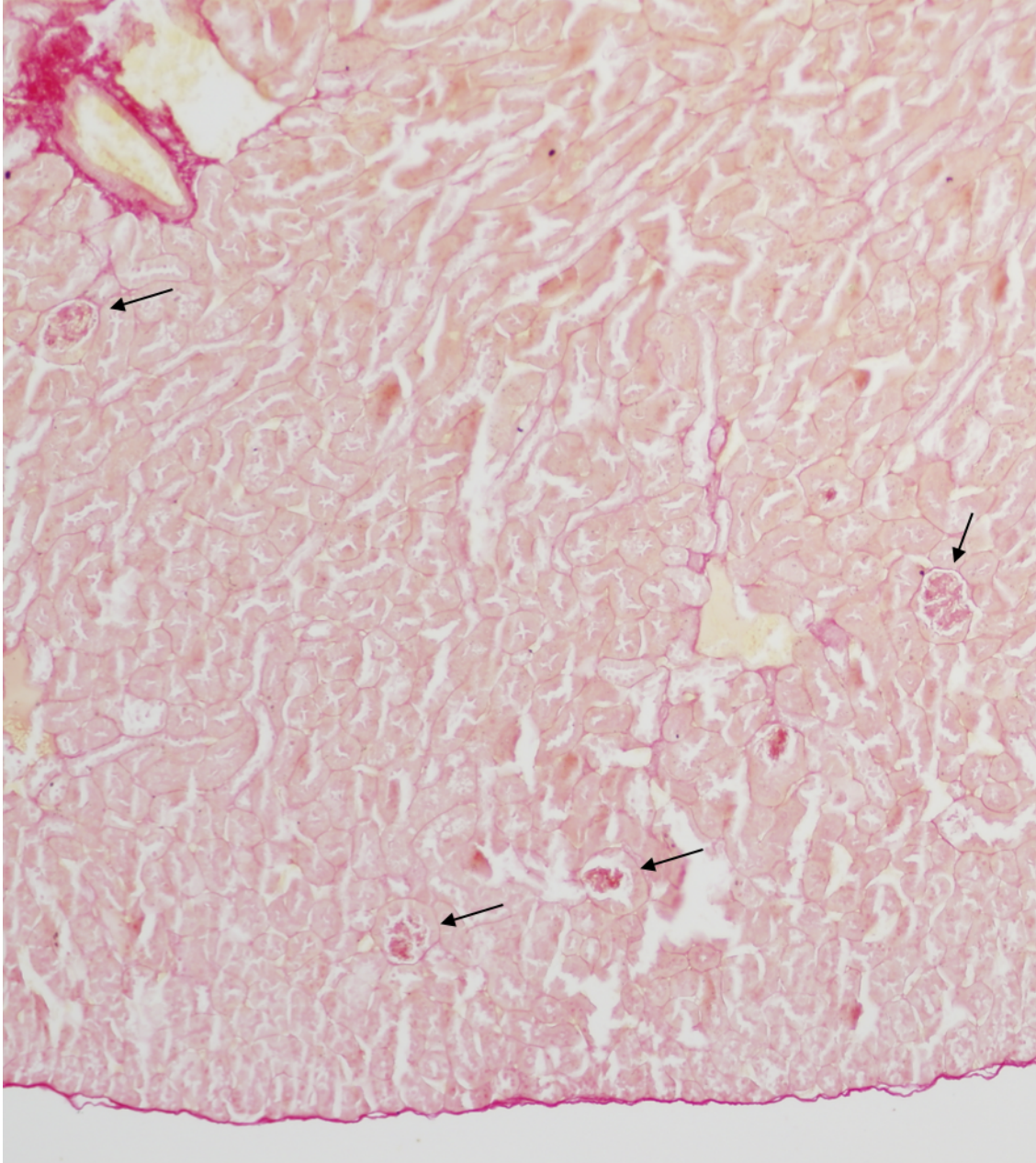


Figure 17. Deposition of Type I Collagen in Untreated Wildtype Mice. Wildtype mice treated with the vehicle IgG and stained with Picrosirius Red. Arrows indicate glomeruli.⁸⁰

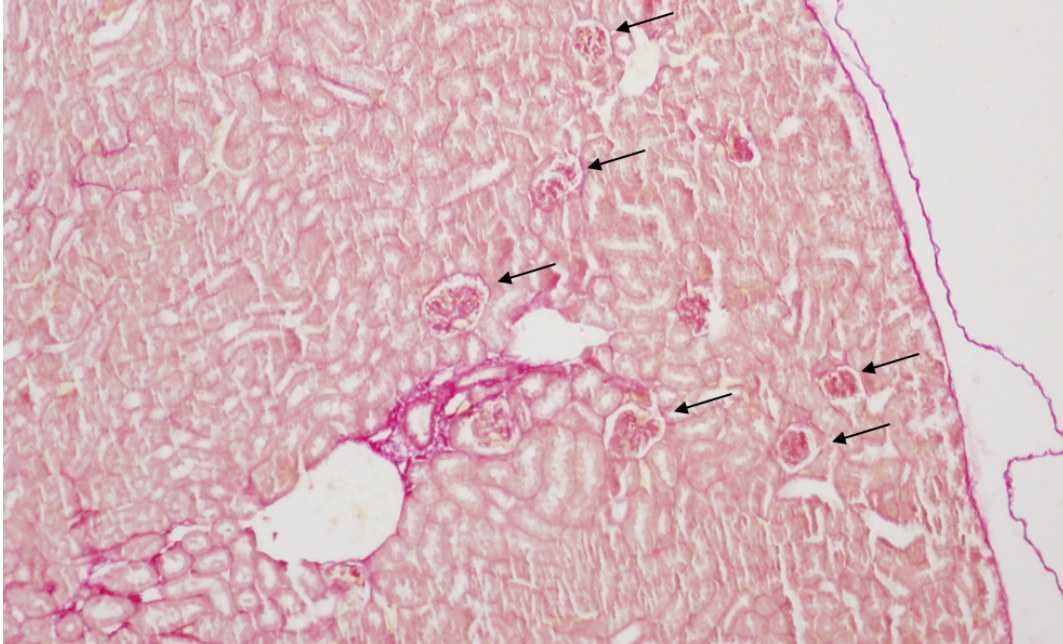


Figure 18. Deposition of Type I Collagen in Treated Wildtype Mice. Wildtype mice treated with the TNF-alpha inhibitor, Etanercept and stained with Picrosirius Red. Arrows indicate glomeruli.⁸⁰

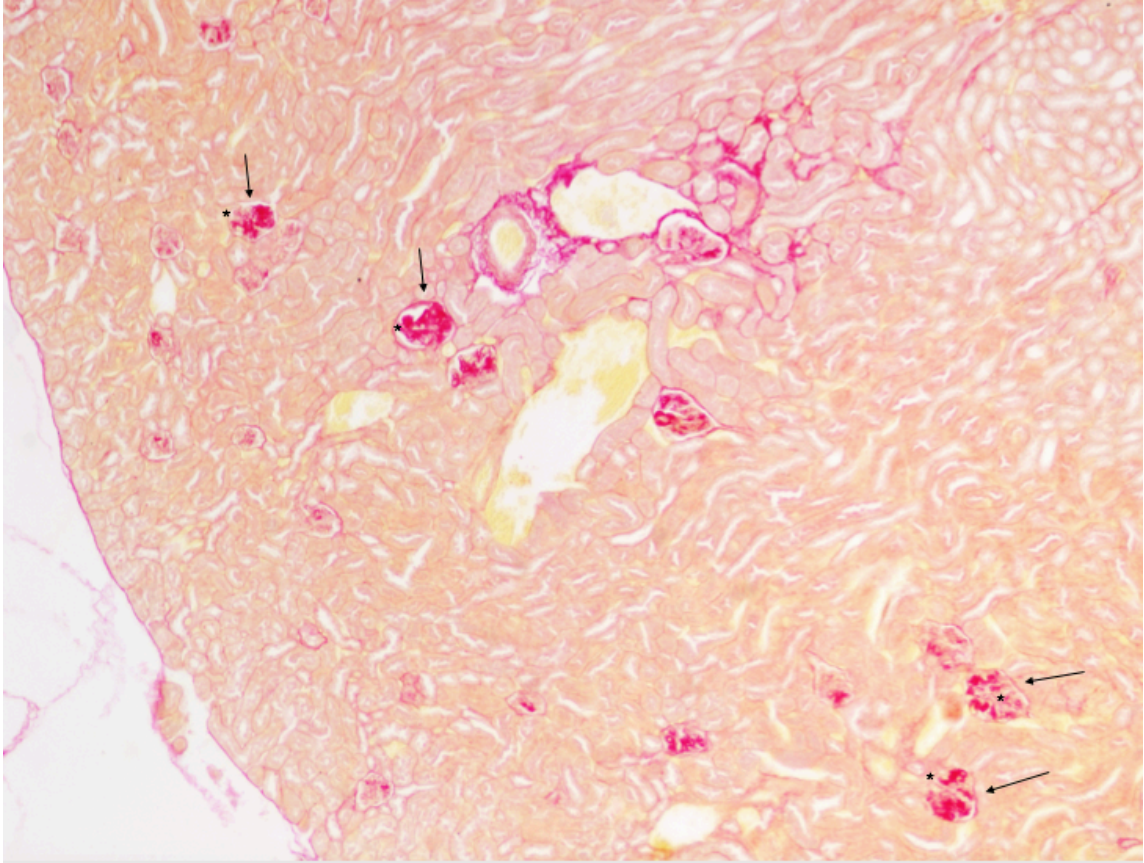


Figure 19. Deposition of Type I Collagen in Untreated *Colla2*-deficient Mice.

Colla2-deficient mice treated with IgG and stained with Picrosirius Red. As expected, there is significant deposition of collagen within the glomeruli. Mean lesion score for affected mice was 3.196 with a p-value of 0.432. Mean difference is significant at the $p < 0.05$ level. Arrows indicate glomeruli. Asterisks indicate moderately severe (G3) to severely (G4) affected and PSR positive glomeruli.⁸⁰

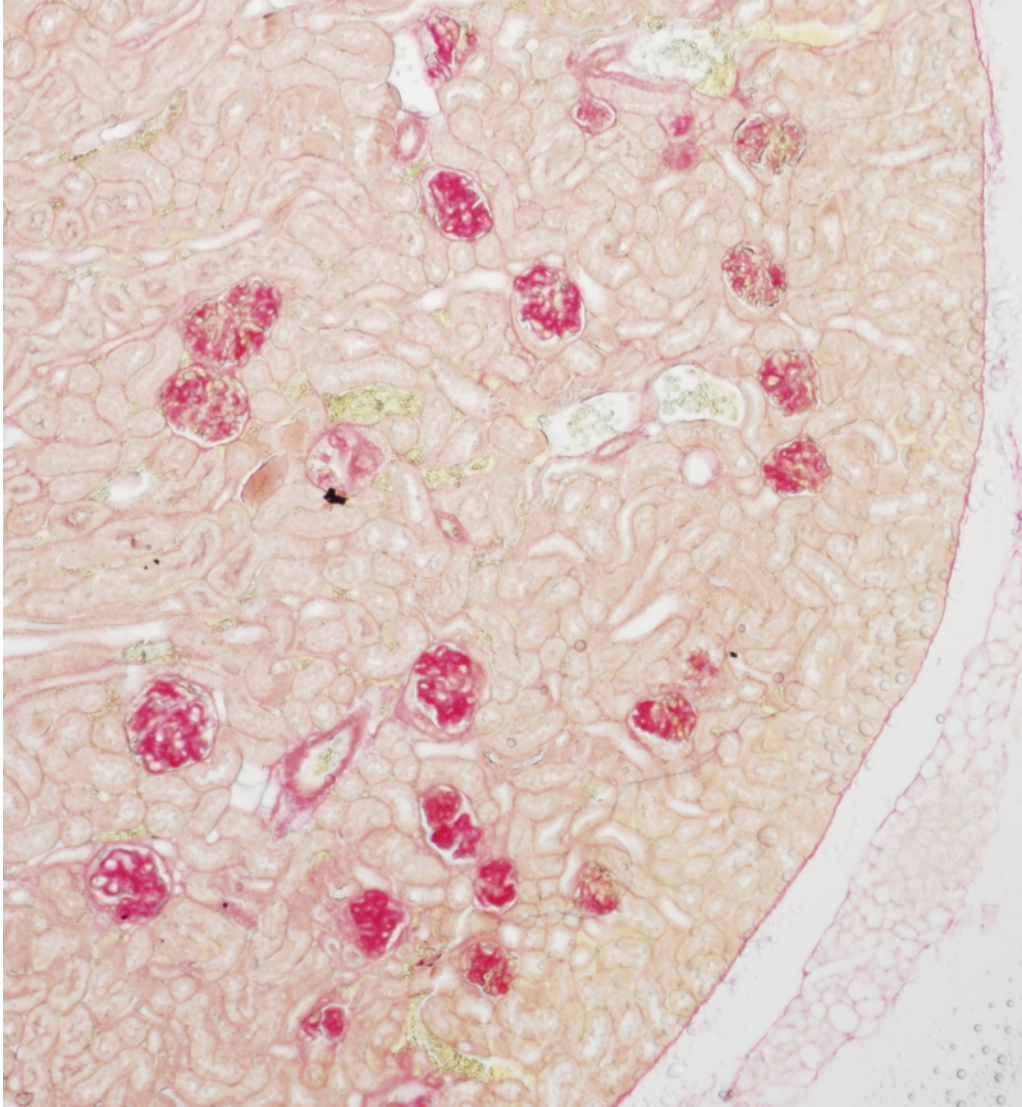


Figure 20. Deposition of Type I Collagen in Treated *Colla2*-deficient Mice. *Colla2*-deficient mice treated with Etanercept and stained with Picrosirius Red. Visually, glomeruli appear to be filled with similar collagen depositions as those treated with the vehicle despite TNF- α inhibition. Mean lesion score for affected mice was 2.799 with a p-value of 0.432. Mean difference is significant at the $p < 0.05$ level. Arrows indicate glomeruli. Asterisks indicate moderately severe to severely affected and PSR positive glomeruli.⁸⁰

Table 2. Mean Lesion Score for Wild Type and *Colla2*-deficient Mice.⁸⁰

Mean Lesion Score					
Genotype	Wildtype + vehicle	Wildtype + Etanercept	<i>Colla2</i> - <i>deficient</i> + vehicle	<i>Colla2</i> - <i>deficient</i> + Etanercept	p-value
Wildtype + vehicle	0	0.046 ± 0.038	3.197 ± 0.191	2.799 ± 0.170	0.000
Wildtype + Etanercept	0.046 ± 0.038	0	3.151 ± 0.195	2.753 ± 0.174	0.000
<i>Colla2</i> - <i>deficient</i> + vehicle	3.197 ± 0.191	3.151 ± 0.195	0	0.398 ± 0.256	0.432
<i>Colla2</i> - <i>deficient</i> + Etanercept	2.799 ± 0.170	2.753 ± 0.174	0.398 ± 0.256	0	0.432

Platelet Derived Growth Factor – Receptor $\beta\beta$, Ligand -BB, Ligand -DD

The second aim of this study was to determine if there is differential labeling, via IHC, of PDGF-BB, PDGF-DD, and PDGFR- $\beta\beta$ in the *Colla2*-deficient mouse model in comparison to the wild type mice. The goal of this aim was to determine if PDGF is the primary mediating molecule in homotrimeric type I collagen glomerulopathy in the *Colla2-deficient* mouse model. It was hypothesized that PDGFR- $\beta\beta$, PDGF-BB, and PDGF-DD would show increased labeling in *Colla2-deficient* mice in comparison to their wild type counterparts.

Six-week-old male and female wild type (+/+) and *Colla2-deficient* (-/-) mice were used for this study. Five wild type (+/+) and five *Colla2-deficient* (-/-) mice were chosen and used for PSR and all IHC runs. Consistent with previous studies, the *Colla2-deficient* mice (-/-) showed homotrimeric type I collagen deposition within glomeruli and no deposition in that of their wild type (+/+) counterparts when evaluated via PSR staining (Figure 21). A morphometry score was assigned to each *Colla2-deficient* (-/-) mouse and is seen in the upper left-hand corner of each section image, with morphometry scores range from 1.8-3.0 (Figure 21). PSR was performed to compare the severity of morphometry score to the intensity of labeling, via IHC, for the different PDGF isoforms.

PDGFR- $\beta\beta$ labeling via IHC showed differential labeling of *Colla2-deficient* mice (-/-) in comparison to wild type mice (+/+) with localization of labeling occurring in the renal mesangium or in the renal epithelium, i.e. podocytes (Figure 22). There was an even distribution of stain evenly spaced throughout the glomeruli in the *Colla2-deficient* mice (-/-) with little, if any stain present in the wild type mice (+/+) (Figure 22). For *Colla2-deficient* mice (-/-), morphometry score increases from left to right (Figure 21)

and labeling of PDGFR- $\beta\beta$ also increases from left to right (Figure 22). The glomeruli with morphometry score 1.8 (Figure 21) and the corresponding glomeruli in Figure 22 (top row, far left) has the least labeling for PDGFR- $\beta\beta$. This is contrasted by the glomeruli with a morphometry score of 3.0 (Figure 21) and its corresponding glomeruli in Figure 22 (top row, far right) has the greatest amount of labeling for PDGFR- $\beta\beta$. These results suggest a positive correlation between morphometry score (lesioning) and the presentation of PDGFR- $\beta\beta$.

PDGF-BB labeling via IHC showed differential labeling of *Colla2-deficient* mice (-/-) in comparison to wild type mice (+/+) with localization of labeling occurring in the renal mesangium or in the renal epithelium, i.e. podocytes (Figure 23). There is stain even distribution throughout the glomeruli in the *Colla2-deficient* mice (-/-) with little if any, stain present in the wild type mice (+/+). For *Colla2-deficient* mice (-/-), morphometry score increases from left to right (Figure 21) and labeling of PDGF-BB also increases from left to right (Figure 23). This is shown by the glomeruli with a morphometry score of 3.0 (Figure 21) and its corresponding glomeruli in Figure 23 (top row, far right) has the greatest amount of labeling for PDGF-BB. These results may represent a relationship between morphometry score (lesioning) and the presentation of PDGF-BB.

PDGF-DD labeling of *Colla2-deficient* mice (-/-) in comparison to their wild type counterparts (+/+) was less conclusive. There was labeling in both *Colla2-deficient* mice (-/-) and wild type mice (+/+) (Figure 24). There was less correlation of morphometry score (Figure 21) and the intensity of labeling for PDGF-DD (Figure 24). For example, the glomeruli with morphometry score 2.3 and 2.9 (Figure 21) mild-severe lesioning had

the greatest amount of stain for PDGF-DD (Figure 24), but the glomeruli corresponding to the morphometry score 3.0 glomeruli had less stain (Figure 24). The inconsistency of labeling in the *Colla2-deficient* mice (-/-) along with the presentation of stain in wild type mice (+/+) make the findings for PDGF-DD inconclusive. There does not seem to be a correlation between morphometry score and intensity of labeling (Figure 21 and 24) or differential labeling when comparing *Colla2-deficient* mice (-/-) to that of their wild type counterparts (+/+) (Figure 24).

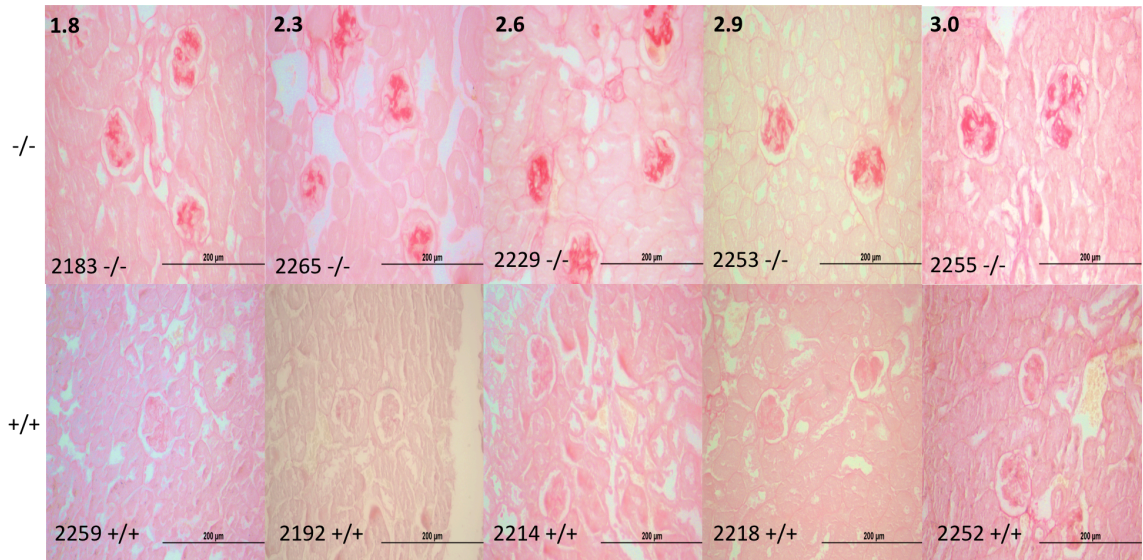


Figure 21. Picosirius Red (PSR) Stain of Five Wild Type and Five *Colla2*-deficient Mice. The top row corresponds to the five *Colla2*-deficient mice (-/-) and the bottom row corresponds to the five wild type mice (+/+). A morphometry score was given to the sections 2183, 2265, 2229, 2253, and 2255. Their associated morphometry scores are 1.8, 2.3, 2.6, 2.9, and 3.0 respectively. Wild type mice are not given a morphometry because no collagen is present within wild type glomeruli.

Beta Receptor 40x

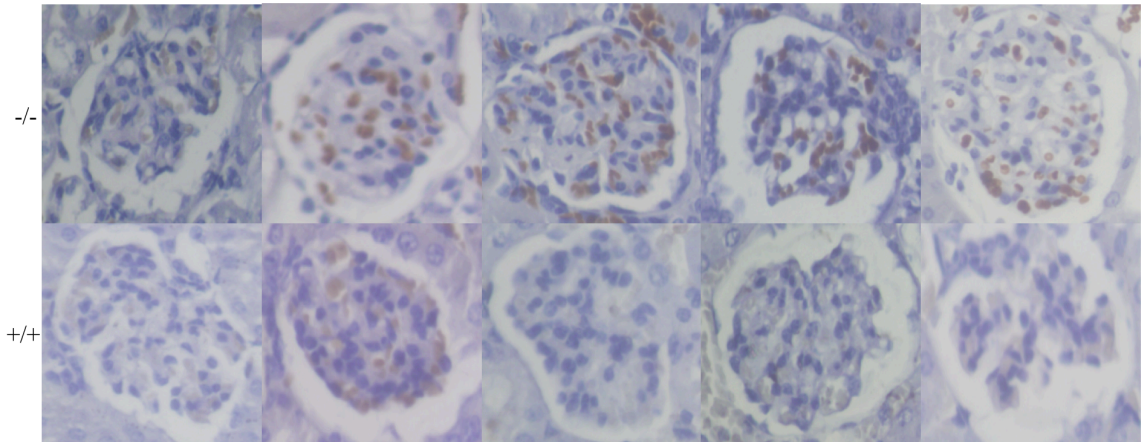


Figure 22. 40x Magnification of PDGFR- $\beta\beta$ Labeling in Glomeruli of Wild Type and *Colla2*-deficient Mice. The top row corresponds to the five *Colla2*-deficient mice (-/-) and the bottom row corresponds to the five wild type mice (+/+). Order of *Colla2*-deficient (-/-) mice corresponds to the order in Figure 22 (2183, 2265, 2229, 2253, and 2255).

PDGF-BB 40x

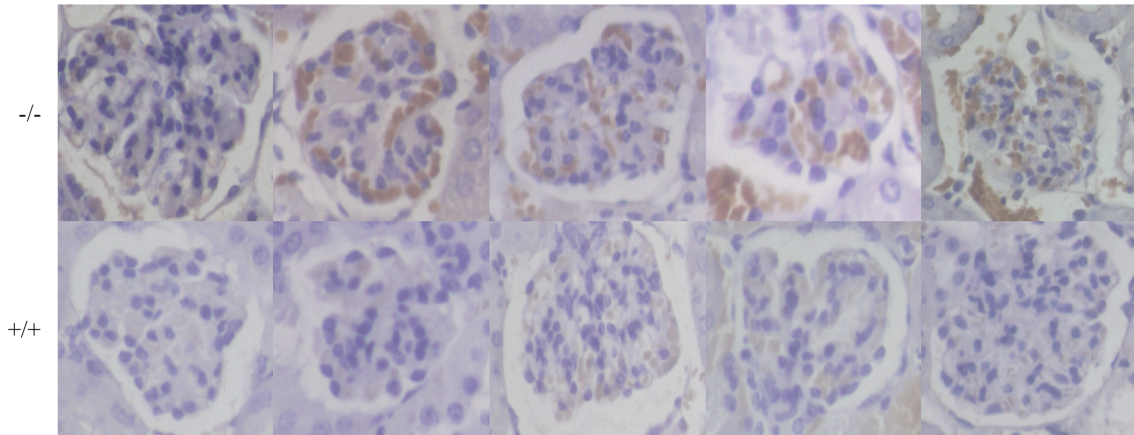


Figure 23. 40x Magnification of PDGF-BB Labeling in Glomeruli of Wild Type and *Colla2*-deficient Mice. The top row corresponds to the five *Colla2*-deficient mice (-/-) and the bottom row corresponds to the five wild type mice (+/+). Order of *Colla2*-deficient (-/-) mice corresponds to the order in Figure 22 (2183, 2265, 2229, 2253, and 2255).

PDGF-DD 40x

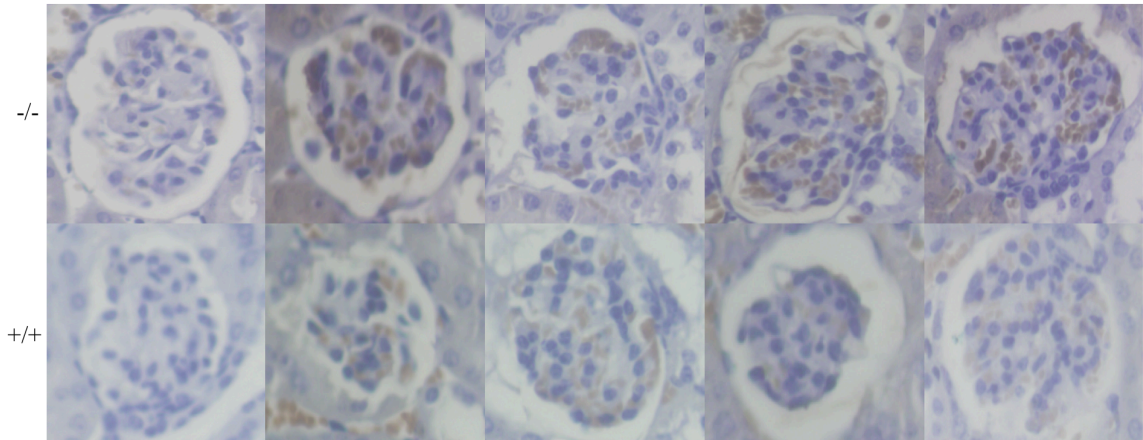


Figure 24. 40x Magnification of PDGF-DD Labeling in Glomeruli of Wild Type and *Colla2*-deficient Mice. The top row corresponds to the five *Colla2*-deficient mice (-/-) and the bottom row corresponds to the five wild type mice (+/+). Order of *Colla2*-deficient (-/-) mice corresponds to the order in Figure 22 (2183, 2265, 2229, 2253, and 2255).

Discussion

Tumor Necrosis Factor – alpha

Tumor Necrosis Factor-alpha (TNF- α) was assessed as a possible contributor to this homotrimeric type I collagen glomerulopathy. As expected, no collagen deposition was seen in wildtype animals consistent with previous work. There is evidence of significant collagen deposition in both *Colla2-deficient* treated (Etanercept) and untreated models (Vehicle IgG). After statistical analysis, there was no significant difference between *Colla2-deficient* mice that received treatment (Etanercept) and *Colla2-deficient* mice that received vehicle (IgG). There were also no significant changes in wildtype mice that received treatment (Etanercept) and wild type mice that received vehicle (IgG). The conclusion of this study was that Etanercept did not affect lesioning within glomeruli, therefore, TNF- α was not the main mediator of collagen deposition in the renal mesangium in the *Colla2-deficient* mouse model.

A limitation of this study is that collagen in this model is present as early as two-weeks of age in *Colla2-deficient* mice and Etanercept was administered twice weekly for six-weeks. With the progressiveness of homotrimeric type I collagen glomerulopathy, Etanercept treatment, may not have been sufficient in diminishing this response. Previous studies have demonstrated that the collagen deposition seen in our model occurs post-natally and as early as two-weeks of age.⁷ This study provides insight at the six-week mark, long after the deposition is known to ensue.⁸⁰

Inflammation is a main event leading to the production and increase of serum TNF- α levels, as well as other cytokines. Furthermore, TNF- α is a proinflammatory

molecule that has activation effects on endothelial cells and activation of multiple cytokines.⁸¹ It has also been shown that TNF- α /TNFR inhibition with neutralizing antibodies and soluble TNFR can decrease protein urea in anti-GBM rat models.⁸² In the *Colla2-deficient* inflammation does not occur as would normally occur in fibrotic conditions. This is a potential limitation as TNF- α /TNFR pathways are characterized by their known proinflammatory effects in fibrosis.

In addition, collagen deposition in bone has been shown to be disrupted by TNF- α . This is due to downregulation in lysyl oxidase, an enzyme responsible for forming crosslinks in type I collagen chains. TNF- α is thereby regulating collagen deposition with little effect on the synthesis of the heterotrimer.⁸³ Interestingly enough, our model for *Colla2-deficient* mice exclusively produce homotrimeric type I collagen. Therefore, it could be suggested that TNF- α is responsible in decreased deposition of the heterotrimer but not the homotrimer or has diminished effects on homotrimeric type I collagen.

Platelet-Derived Growth Factor

PDGFR- $\beta\beta$, PDGF-BB, and PDGF-DD were evaluated to determine the primary mediators of homotrimeric type I collagen glomerulopathy. It was found, as in previous studies, that homotrimeric collagen deposition is occurring in *Colla2-deficient* mice when evaluated via PSR. Furthermore, it was also found, as in previous studies, that no homotrimeric type I collagen is being deposited in wild type mice. Evaluation of labeling via IHC showed differential labeling for PDGFR- $\beta\beta$ and PDGF-BB, contrasted by less conclusive labeling for PDGF-DD. PDGF-DD was the only stain present in glomeruli of wild type mice. Morphometry mapping, assessed via PSR, correlated to IHC labeling

intensity for PDGFR- $\beta\beta$ and PDGF-BB, but was unrelated in the labeling via IHC for PDGF-DD.

Differential labeling for the different isoforms of PDGF would be expected when comparing wild type mice to that of their *Colla2-deficient* counterparts. This is due to the involvement of PDGF in renal disease, proliferation, cell survival, cell migration, and the production of ECM.⁶¹ The collagen deposition seen in *Colla2-deficient* mice is hypothesized as a result of the secondary wound healing response as the body responds to kidney injury or damage.⁷ PDGF has been shown to be upregulated in many forms of renal fibrotic mouse models⁶¹ therefore, it is suggested that it would also be upregulated in the *Colla2-deficient* mouse model. Further study is needed to definitively say if PDGF-receptor/ligand interaction is the main mediator of collagen deposition in the *Colla2-deficient* mouse model, thereby, being the main mediator of the secondary wound healing response.

A new study looks at fucosylation as a potential mediator of renal fibrosis as it has been shown to regulate alpha-smooth muscle actin (α -SMA), a known marker of myofibroblast proliferation, thereby, an indicator of fibrosis.

Core Fucosylation Regulation – PDGF & TGF- β 1

Fucosylation is the process by which fucose groups are added to N-terminal glycans on receptors by enzymes known as fucosyltransferase (FUT) (Figure 4 in Appendix).

A recent study in 2017 looked at FUT8 knockdowns via siRNA and shRNA to see if their regulation had implications on fibrotic effects of unilateral ureteral obstruction (UUO) mouse models, specifically regulation of PDGF-receptors and TGF- β 1

receptors.⁷⁹ Their results show that they could alleviate α -SMA expression and myofibroblastic morphological changes in pericytes upon knockdown of FUT8 (Figure 1A&B in Appendix). Furthermore, it was shown that siRNA for FUT8 could successfully knockdown FUT8/LCA expression (Figure 1C in Appendix).⁷⁹

Histological examination of tissue in this study also showed UUO fibrotic tissue in UUO day seven mice, however, when these mice were treated with siRNA for FUT8 tissue was dramatically less scarred and damaged (Figure 2A in Appendix). It was further shown, via immunofluorescence that α -SMA could be alleviated upon induction with siRNA for FUT8 (Figure 2B in Appendix).⁷⁹ Finally, they did a protein quantification for PDGF and TGF- β 1 receptors along with their downstream mediators ERK and smad2/3 respectively. It was shown that immunoprecipitated LCA bound to both receptors was down regulated in mice treated with siRNA for FUT8, as well as, a decrease in the downstream mediators for both receptors (Figure 3 in Appendix).⁷⁹

Future Directions

Further investigation is required to assess the role of TNF- α in the early stages of homotrimeric type I collagen glomerulopathy in *Colla2-deficient* mice, as well as, the potential correlation between epithelial-to-mesenchymal transition and TNF- α in *Colla2-deficient* mice. A limitation of this TNF- α study was the age and dryness of kidney sections, therefore, it is suggested that further experiments be done to confirm the findings reported on this study. This could include RT-PCR for mRNA transcripts of TNF- α and western blotting to see if there is differential expression of mRNA and protein in comparison of wild type mice and that of their *Colla2-deficient* counterparts.

The initial results from IHC for PDGFR- $\beta\beta$, PDGF-BB, and PDGF-DD show promise as potentially leading to homotrimeric type I collagen glomerulopathy, however, RT-PCR will need to be performed to confirm expression of mRNA for PDGFR- $\beta\beta$, PDGF-BB, and PDGF-DD, as well as, Western blot for PDGFR- $\beta\beta$, PDGF-BB, and PDGF-DD to confirm if protein expression is upregulated in response to mRNA. This may need to be followed up by a study of PDGF-AA, PDGF-CC, and PDGFR- $\alpha\alpha$ as well.

Finally, a new study has shown how regulation of core fucosylation can have effects on α -SMA expression, PDGFR activation, and TGF- β 1 receptor activation.⁶⁹ It would be interesting to apply core fucosylation regulation to the *Colla2-deficient* mouse model to see if PDGF receptor and TGF- β 1 receptor activation is synergistically leading to homotrimeric type I collagen glomerulopathy in the *Colla2-deficient* mouse model.

REFERENCES

1. Center for Disease Control (CDC). National chronic kidney disease fact sheet, 2017. <https://www.cdc.gov/kidneydisease/pdf/kidneyfactsheet.pdf>. Accessed April 15, 2018.
2. Chronic kidney disease. 2018, March 08. <https://www.mayoclinic.org/diseases-conditions/chronic-kidney-disease/>. Accessed April 15, 2018.
3. United States Renal Data System (USRDS). Highlights from the USRDS 2017 annual data report.
4. Phillips CL, Pfeiffer BJ, Luger AM, Franklin CL. Novel collagen glomerulopathy in a homotrimeric type I collagen mouse (oim). *Kidney Int.* 2002;62(2),383-391.
5. Steiner RD, Adsit J, Basel D. COL1A1/2-Related osteogenesis imperfecta. 2005 Jan 28 [Updated 2013 Feb 14]. In: Adam MP, Ardinger HH, Pagon RA, et al., editors. GeneReviews® [Internet]. Seattle (WA): University of Washington, Seattle; 1993-2018. Available from:<https://www.ncbi.nlm.nih.gov/books/NBK1295/>
6. Lodish H, Berk A, Zipursky SL, et al. Molecular Cell Biology. 4th edition. New York: W. H. Freeman; 2000. Section 22.3, Collagen: The fibrous proteins of the matrix. Available from: <https://www.ncbi.nlm.nih.gov/books/NBK21582/>
7. Brodeur AC, Wirth DA, Franklin CL, et al. Type I collagen glomerulopathy: postnatal collagen deposition follows glomerular maturation. *Kidney Int.* 2007;71(10):985-993.
8. Wu C, Walton C, Wu G. Propeptide-mediated regulation of pro collagen synthesis in IMR-90 human lung fibroblast cell cultures. *J Biol Chem.* 1991;266,2983-2987.
9. Marini JC. et al. Osteogenesis imperfecta. *Nat. Rev. Dis. Primers* 2017. doi:10.1038/nrdp.2017.52
10. Col1a2 collagen, type I, alpha 2 [Mus musculus (house mouse)] - Gene - NCBI. (n.d.). <https://www.ncbi.nlm.nih.gov/gene/12843>. Accessed April 15, 2018.
11. Col1a1 collagen, type I, alpha 1 [(house mouse)]. (n.d.). <https://www.ncbi.nlm.nih.gov/gene/12842>. Accessed April 15, 2018.
12. Kielty C, Hopkinson I, Grant M. Connective tissues and its heritable disorders: collagen: the collagen family: structure, assembly and organization in the extracellular matrix. 1993. New York, NY: Wiley-Liss
13. Prockop DJ, Fertala A. Inhibition of the self-assembly of collagen I into fibrils with synthetic peptides. Demonstration that assembly is driven by specific binding sites on the monomers. *J Biol Chem.* 1998;273(25),15598-15604.
14. Roberts-Pilgrim AM, Makareeva E, Myles MH, et al. Deficient degradation of homotrimeric type I collagen, alpha1 (I)(3) glomerulopathy in oim mice. *Mol Genet Metab.* 2011;104(3),373–382.

15. Bachinger HP, Mizuno K, Vranka J, Boudko SP. in *Comprehensive Natural Products II: Chemistry and Biology* (eds Mander, L. & Liu, H.-W.) 469–530 (Elsevier Ltd, 2010).
16. Colige A. et al. cDNA cloning and expression of bovine procollagen I N-proteinase: a new member of the superfamily of zinc-metalloproteinases with binding sites for cells and other matrix components. *Proc. Natl Acad. Sci. USA* 1997;94,2374–2379.
17. Ballermann BJ. Glomerular endothelial cell differentiation. *Kidney Int.* 2005;67(5), 1668-1671. doi:10.1111/j.1523-1755
18. Reiser J, Altintas MM. Podocytes. F1000Research. 2006. doi:10.12688/f1000research.7255.1
19. Scindia Y, Deshmukh U, Bagavant H. Mesangial pathology in glomerular disease: targets for therapeutic intervention. *Advanced Drug Deliv. Rev.* 2010;62 (14): 1337–1343. doi:10.1016/j.addr.2010.08.011. PMC 2992591. PMID 20828589.
20. Scheinman J, Yanaka H, Haralson M. Specialized collagen mRNA and secreted collagens in human glomerular epithelial, mesangial, and tubular cells. *J Am Soc Nephrol.* 1992;2,1475-1483.
21. Schlondorff D. The glomerular mesangial cell: An expanding role for a specialized pericyte. *FASEB Journal.* 1987;1(4),272-281.
22. Murawski IJ, Maina RW, Gupta IR. The relationship between nephron number, kidney size and body weight in two inbred mouse strains. *Organogenesis,* 2010;6(3),189–194.
23. Andrews KL, Betsuyaku T, Rogers S, et al. Gelatinase B (MMP-9) is not essential in the normal kidney and does not influence progression of renal disease in a mouse model of alport syndrome. *Am J Path.* 2000;157(1),303–311.
24. Spitzer A, Brandis M. Functional and morphologic maturation of the superficial nephrons relationship to total kidney function. *J Clin Inv.* 1974;53(1),279–287.
25. Kleinman LI, Reuter JH. Maturation of glomerular blood flow distribution in the new-born dog. *J Physiol.* 1973;228(1),91–103.
26. Potter EL. Development of the human glomerulus. *Arch Pathol* 1965;80:241-255.
27. Aperia A, Herin P. Development of glomerular perfusion rate and nephron filtration rate in rats 17-60 days old. *Am J Physiol* 1975;228:1319-1325.
28. The Editors of Encyclopedia Britannica. 2007, November 13. Nephron.
29. Doig A, Huether S. Structure and Function of the Renal and Urologic Systems. 2016, September 09.
30. Haralson MA, Jacobson HR, Hoover RL. Collagen polymorphism in cultured rat kidney mesangial cells. *Lab Inv.* 1987;57:513–523.

31. Sanderson N, Factor V, Nagy P, et al. Hepatic expression of mature transforming growth factor beta 1 in transgenic mice results in multiple tissue lesions. *Proceedings of the National Academy of Sciences*. 1995;92(7),2572-2576.
32. Kopp J, Factor V, Mozes M, et al. Transgenic mice with increased plasma levels of TGF-beta 1 develop progressive renal disease. *Lab Inv*. 1996;74,991-1003.
33. Burke M, Pabbidi M, Farley J, Roman R. Molecular mechanisms of renal blood flow autoregulation. *Current Vascular Pharmacology CVP*, 2014;12(6),845-858.
34. Yu Q, Stamenkovic I. Cell surface-localized matrix metalloproteinase-9 proteolytically activates TGF-beta and promotes tumor invasion and angiogenesis. *Genes Dev*, 2000;14,163-176.
35. Zhan M, Kanwar YS. Hierarchy of molecules in TGF- 1 signaling relevant to myofibroblast activation and renal fibrosis. *AJP: Renal Physiology*, 2014;307(4),F385-F387.
36. Fu R, Wu J, Xue R, et al. Premature senescence and cellular phenotype transformation of mesangial cells induced by TGF-B1. *Renal Failure*, 2013;35(8),1142-1145.
37. Meng X, Tang PM, Li J, Lan HY. TGF-B/Smad signaling in renal fibrosis. *Frontiers in Physiology Front. Physiol.*, 2015;6.
38. Liu Y. Renal fibrosis: new insights into the pathogenesis and therapeutics. *Kidney Int*. 2006;69:213-217.
39. Yeh YC, Wei WC, Wang YK, et al. Transforming growth factor- β 1 induces Smad3-dependent β 1 integrin gene expression in epithelial-to-mesenchymal transition during chronic tubulointerstitial fibrosis. *Am J Pathol*. 2010;177:1743-1754.
40. Barnes JL, Gorin Y. Myofibroblast differentiation during fibrosis: role of NAD(P)H oxidases. *Kidney Int*. 2011;79:944-956.
41. Zhao H. Matrix metalloproteinases contribute to kidney fibrosis in chronic kidney diseases. *World J Neph WJN*, 2013;2(3),84.
42. O'Connor JW, Gomez EW. Biomechanics of TGF β -induced epithelial-mesenchymal transition: Implications for fibrosis and cancer. *Clin Transl Med*. 2014;3(1),23-36.
43. Romero D, Al-Shareef Z, Gorroño-Etxebarria I, et al. Dickkopf-3 regulates prostate epithelial cell acinar morphogenesis and prostate cancer cell invasion by limiting TGF- β -dependent activation of matrix metalloproteinases. *Carcinogenesis*, 2015;37(1),18-29.
44. Fragiadaki M, Mason RM. Epithelial-mesenchymal transition in renal fibrosis - evidence for and against. *Int. J Exp Pathol*. 2011;92(3),143-150.
45. Willis BC, Borok Z. TGF-beta-induced EMT: mechanisms and implications for fibrotic lung disease. *Am J Physiol: Lung cellular and molecular physiology* 2007;293:L525-534.

46. Bariety J. Glomerular epithelial-mesenchymal transdifferentiation in pauci-immune crescentic glomerulonephritis. *Neph Dial Trans.* 2003;18(9),1777-1784.
47. Hinz B. Formation and function of the myofibroblast during tissue repair. *J Inv Derm.* 2007;127(3),526-537.
48. Tian Y, Fraser D, Attisano L, Phillips AO. TGF- β 1-mediated alterations of renal proximal tubular epithelial cell phenotype. *Am J Physiol. Renal Physiol.* 2003;285(1),F130-F142.
49. Rastaldi, MP, Ferrario F, Giardino L, et al. Epithelial-mesenchymal transition of tubular epithelial cells in human renal biopsies. *Kidney Int.* 2002;62(1),137-146.
50. PCNA proliferating cell nuclear antigen [Homo sapiens (human)] - Gene - NCBI. (n.d.). <https://www.ncbi.nlm.nih.gov/gene>. Accessed April 15, 2018.
51. Brodeur AC, Roberts-Pilgrim AM, Thompson KL, et al. Transforming growth factor- β 1/smad3-independent epithelial-mesenchymal-transition in type I collagen glomerulopathy. *Int J Nephrol Renovasc Dis.* 2017;10:251-259.
52. Baud L, Fouqueray B, Philippe C, Amrani A. Tumor necrosis factor alpha and mesangial cells. *Kidney Int.* 1992;41(3),600-603.
53. Koukouritaki S, Vardaki E, Papakonstanti E, et al. TNF-alpha induces actin cytoskeleton reorganization in glomerular epithelial cells involving tyrosine phosphorylation of paxillin and focal adhesion kinase. *Mol Med.* 1999;5(6),382-392.
54. Ryu M, Mulay SR, Miosge N, Gross O, Anders H. Tumour necrosis factor- α drives Alport glomerulosclerosis in mice by promoting podocyte apoptosis. *J Pathol.* 2011;226(1),120-131.
55. Chuang M, Sun K, Tang S, et al. Tumor-derived tumor necrosis factor-alpha promotes progression and epithelial-mesenchymal transition in renal cell carcinoma cells. *Cancer Science*, 2008;99(5),905-913.
56. Chung CH, Fan J, Lee EY, et al. Effects of tumor necrosis factor- α on podocyte expression of monocyte chemoattractant protein-1 and in diabetic nephropathy. *Nephron Extra* 2015;5(1),1-18.
57. Suranyi MG, Guasch A, Hall BM, Myers BD. Elevated Levels of Tumor Necrosis Factor- α in the Nephrotic Syndrome in Humans. *Am J Kidney Dis.* 1993;21(3),251-259.
58. Madhusudan S. Study of etanercept, a tumor necrosis factor-alpha inhibitor, in recurrent ovarian cancer. *J Clin Oncol.* 2005;23(25),5950-5959.
59. Floege J, Eitner F, Alpers CE. A new look at platelet-derived growth factor in renal disease. *J Am Soc Nephrol* 2008;19:12-23
60. Aiping L, Jie D. Potential role of Akt signaling in chronic kidney disease, *Neph Dial Trans.* 2015;30(3),385-394.
61. Ostendorf T, Eitner F, Floege J. The PDGF family in renal fibrosis. *Pediatr Nephrol.* 2012;27:1041-1050.

62. Floege J, Johnson RJ. Multiple roles for platelet-derived growth factor in renal disease. *Miner Electrolyte Metab* 1995;21:271–282.
63. Heldin CH, Westermark B. Mechanism of action and in vivo role of platelet-derived growth factor. *Physiol Rev* 1999;79:1283–1316
64. Floege J, Eitner F, Van Roeyen C, Ostendorf T. PDGF-D and renal disease: yet another one of those growth factors? *J Am Soc Nephrol* 2003;14:2690–2691
65. Rose BA, Force T, Wang Y. Mitogen-activated protein kinase signaling in the heart: Angels versus demons in a heart-breaking tale. *Physiol Rev.* 2010;90(4).
66. Shirane M, Sawa H, Kobayashi Y, et al. Deficiency of phospholipase C- γ 1 impairs renal development and hematopoiesis. *Development* 2001;128:5173-5180.
67. Bonner JC. Regulation of PDGF and its receptors in fibrotic diseases. *Cytokine & Growth Factor Rev.* 2004;15(4),255-273.
68. Betsholtz C, Lindblom P, Bjarnegard M, et al. Role of platelet-derived growth factor in mesangium development and vasculopathies: Lessons from platelet-derived growth factor and platelet-derived growth factor receptor mutations in mice. *Curr Opin Nephrol Hypertens* 2004;13:45–52.
69. Ding H, Wu X, Bostrom H, et al. A specific requirement for PDGF-C in palate formation and PDGFR-alpha signaling. *Nat Genet.* 2004;36:1111–1116
70. Soriano P. Abnormal kidney development and hematological disorders in PDGF beta- receptor mutant mice. *Genes Dev.* 1994;8:1888–1896
71. Sano H, Ueda Y, Takakura N, et al. Blockade of platelet-derived growth factor receptor-beta pathway induces apoptosis of vascular endothelial cells and disrupts glomerular capillary formation in neonatal mice. *Am J Pathol* 2002;161:135–143
72. Bjarnegard M, Enge M, Norlin J, et al. Endothelium-specific ablation of PDGFB leads to pericyte loss and glomerular, cardiac and placental abnormalities. *Development.* 2004;131:1847–1857
73. Andrae J, Gallini R, Betsholtz C. Role of platelet-derived growth factors in physiology and medicine. *Genes Dev* 2008;22:1276–1312
74. Boor P, Konieczny A, Villa L, et al. PDGF-D inhibition by CR002 ameliorates tubulointerstitial fibrosis following experimental glomerulonephritis. *Nephrol Dial Transplant.* 2007;22:1323–1331
75. Kong D, Li Y, Wang Z, et al. miR-200 regulates PDGF-D-mediated epithelial-mesenchymal transition, adhesion, and invasion of prostate cancer cells. *Stem Cells.* 2009;27:1712–1721
76. Eitner F, Ostendorf T, Van Roeyen C, et al. Expression of a novel PDGF isoform, PDGF-C, in normal and diseased rat kidney. *J Am Soc Nephrol* 2002;13:910–917
77. Taneda S, Hudkins KL, Topouzis S, et al. Obstructive uropathy in mice and humans: Potential role for PDGF-D in the progression of tubulointerstitial injury. *J Am Soc Nephrol.* 2003;14:2544–2555

78. Eitner F, Ostendorf T, Kretzler M, et al. PDGF-C expression in the developing and normal adult human kidney and in glomerular diseases. *J Am Soc Nephrol*. 2003;14:1145–1153
79. Wang N, Deng Y, Liu A, et al. Novel mechanism of the pericyte-myofibroblast transition in renal interstitial fibrosis: Core fucosylation regulation. *Scientific Reports*. 2017;7,16914.
80. Thompson KL. Characterization of the effects of etanercept treatment (TNF- α inhibition) in type I collagen glomerulopathy. Submitted 2017. Graduate Seminar Paper. Missouri State University.
81. Javid B, Quigg RJ. Treatment of glomerulonephritis: Will we ever have options other than steroids and cytotoxics? *Kidney Int*. 2005;67(5),1692-1703.
82. Mulligan MS, Johnson KJ, Todd RF III, et al. Requirements for leukocyte adhesion molecules in nephrotoxic nephritis. *J Clin Invest* 1993;91:557-587.
83. Pischon N, Darbois LM, Palamakumbura AH, et al. Regulation of collagen deposition and lysyl oxidase by tumor necrosis factor- α in osteoblasts. *J Biol Chem*. 2004;279(29),30060-30065.
84. Li L, et al. Inhibiting core fucosylation attenuates glucose-induced peritoneal fibrosis in rats. *Kidney Int*. 2018.

APPENDIX

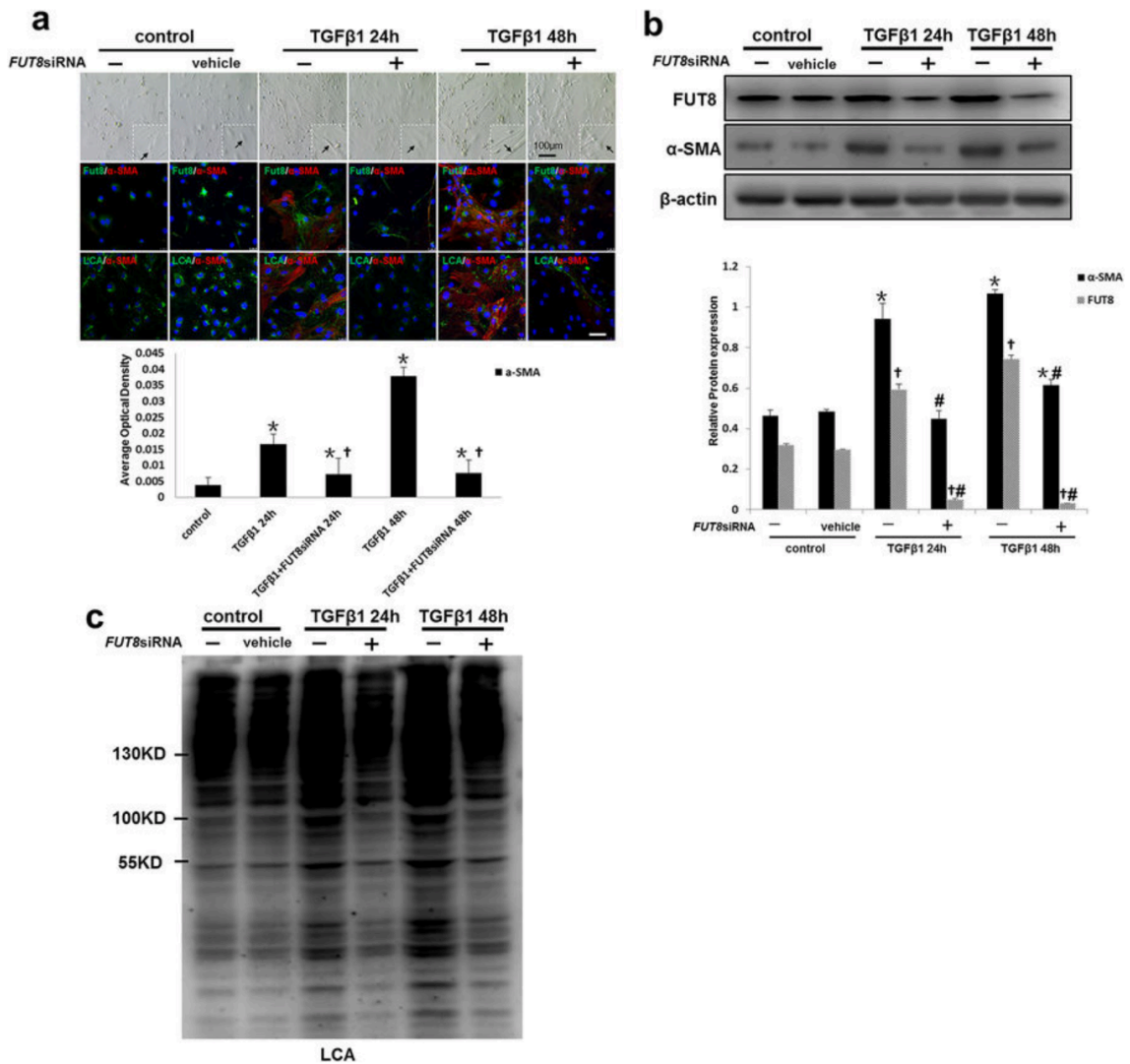


Figure A1. Core fucosylation was down-regulated and the pericyte-myofibroblast transition was inhibited upon FUT8 knockdown *in vitro*. Primary cultures of pericytes were incubated with TGFβ1 (10 ng/ml) for 24 or 48 h. **(a)** Representative bright-field images of morphological changes in pericytes, where black arrows indicate pericytes, and representative images of FUT8 (green), LCA (green), and α-SMA (red) staining are shown. Quantification is shown in the lower panel. **(b)** FUT8 and α-SMA levels were assessed using Western blot analyses. Quantification is shown in the lower panel. **(c)** Lectin blot analyses. Cell lysates were subjected to a lectin blot analysis using LCA. Representative data are shown. Quantification is shown in the lower panel. Scale bar, 50 μm. * $P < 0.01$, † $P < 0.01$. * and † indicate the comparison of the control group with the TGFβ1 group; # indicates the comparison of the FUT8 knockdown group with the TGFβ1 group.⁷⁹

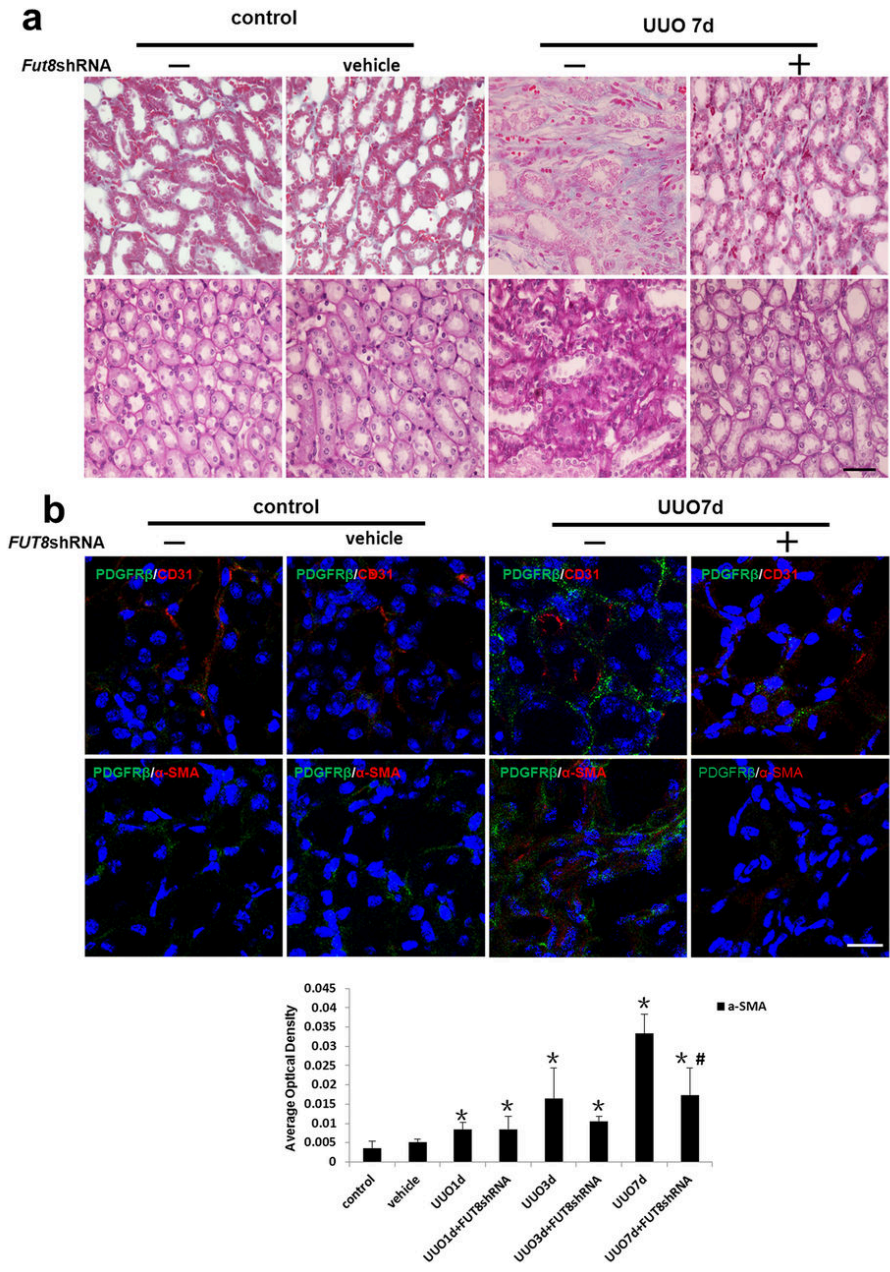


Figure A2. The pericyte-myofibroblast transition was inhibited and RIF was reduced upon FUT8 knockdown *in vivo*. UUO models were established (n = 5). A recombinant adenovirus carrying the *FUT8* shRNA was used to knock down *FUT8* expression *in vivo*. (a) Representative images of Masson's trichrome-stained and PAS-stained UUO kidney sections. (b) Representative images of dual staining for PDGFR β (green) and α -SMA (red) staining and dual staining for PDGFR β (green) and CD31 (red). Quantification of α -SMA staining is shown in the lower panel. Scale bar, 50 μ m. * $P < 0.01$, # $P < 0.01$. *Indicates the comparison of the control group with the UUO group; # indicates the comparison of the *FUT8* knockdown group with the UUO group.⁷⁹

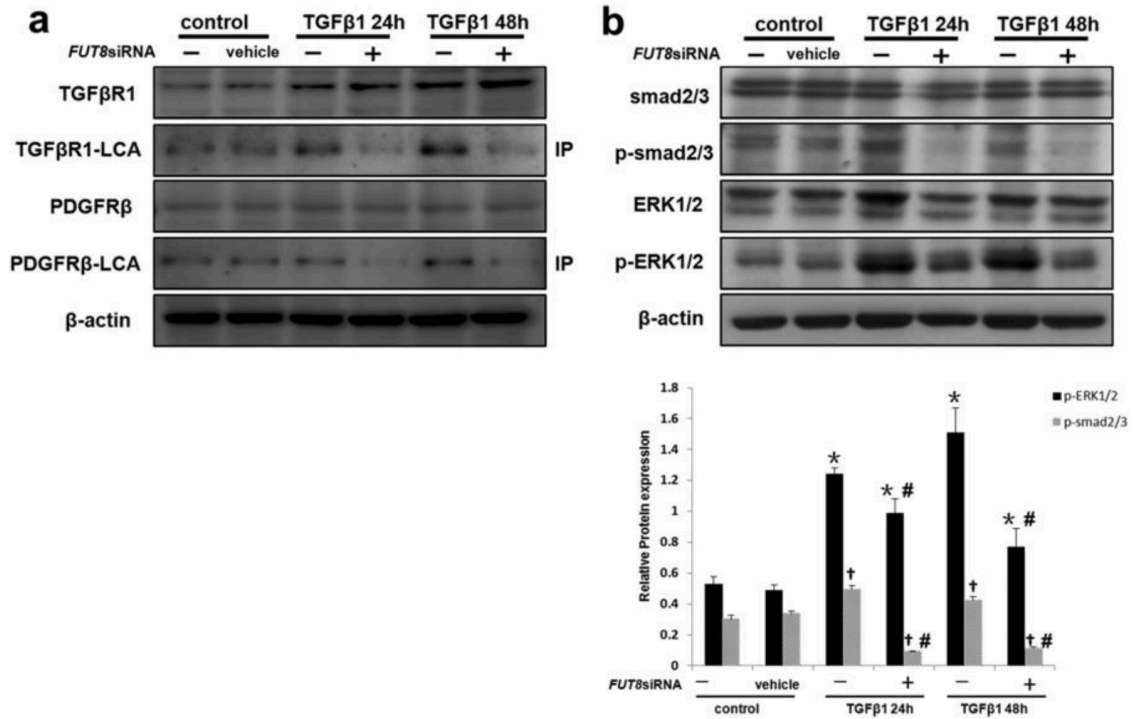


Figure A3. Core fucosylation regulates the pericyte-myofibroblast transition through both the TGFβ/Smad2/3 and PDGF/ERK1/2 pathways *in vitro*. (a) TGFβ1 and PDGFRβ levels in total cell lysates were assessed using Western blot analyses. Lectin blot analysis of the immunoprecipitated TGFβ1 and PDGFRβ proteins. TGFβ1 and PDGFRβ were immunoprecipitated from whole cell lysates with anti-TGFβ1 and anti-PDGFRβ antibodies, respectively. The blots were probed with LCA. Representative data are shown. Quantification is shown in the lower panel. (b) Smad2/3, p-Smad2/3, ERK1/2, and p-ERK1/2 levels were assessed using Western blot analyses. Total cell lysates were subjected to immunoblotting. Representative data are shown. Quantification is shown in the lower panel. * $P < 0.01$, # $P < 0.01$. * and † indicate the comparison of the control group with the TGFβ1 group; # indicates the comparison of the FUT8 knockdown group with the TGFβ1 group.⁷⁹

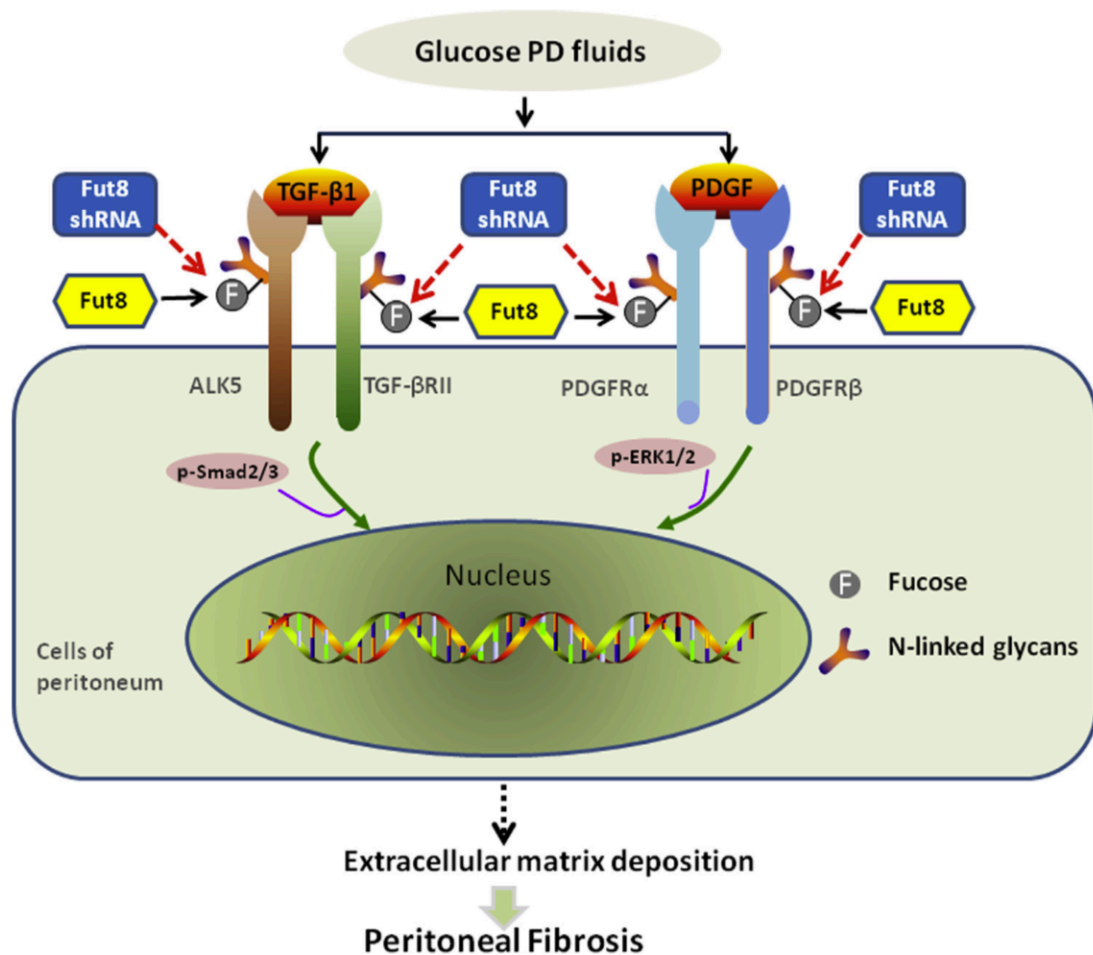


Figure A4. Core fucosylation regulates transforming growth factor b (TGF-b) and platelet-derived growth factor (PDGF) signaling pathways in the pathophysiology of peritoneal fibrosis. Core fucosylation is a common posttranslational modification of key receptors of these signaling pathways, including both TGF-b and PDGF receptors (PDGFRs). Glucose peritoneal dialysis (PD) fluid upregulates core fucosylation, promoting the α -1,6 fucosyltransferase (Fut8) to fucosylate the extracellular domains of TGF-b and PDGF receptors, activate TGF-b/ Smad2/3 and PDGF/ERK signaling, and subsequently induce extracellular matrix deposition, leading to peritoneal fibrosis. Fut8 short hairpin RNA (shRNA) significantly attenuated peritoneal fibrosis in a rat model of peritoneal fibrosis via abrogating core fucosylation of the TGF-b and PDGF receptors. ALK5, activin receptor-like kinase 5; F, fucose; p, phosphorylated; TGF-bRII, TGF-b receptor II.⁸⁴